Accepted Manuscript

Discovery of small-molecule nonpeptide antagonists of nociceptin/orphanin FQ receptor: The studies of design, synthesis, and structure–activity relationships for (4-arylpiperidine substituted-methyl)-[bicyclic (hetero)cycloalkanobenzene] derivatives

Shigeo Hayashi, Katsuyo Ohashi, Sachiko Mihara, Eriko Nakata, Chie Emoto, Atsuko Ohta

PII: S0223-5234(16)30084-8

DOI: 10.1016/j.ejmech.2016.02.014

Reference: EJMECH 8365

To appear in: *European Journal of Medicinal Chemistry*

Received Date: 11 May 2015

Revised Date: 6 January 2016

Accepted Date: 4 February 2016

Please cite this article as: S. Hayashi, K. Ohashi, S. Mihara, E. Nakata, C. Emoto, A. Ohta, Discovery of small-molecule nonpeptide antagonists of nociceptin/orphanin FQ receptor: The studies of design, synthesis, and structure–activity relationships for (4-arylpiperidine substituted-methyl)-[bicyclic (hetero)cycloalkanobenzene] derivatives, *European Journal of Medicinal Chemistry* (2016), doi: 10.1016/j.ejmech.2016.02.014.

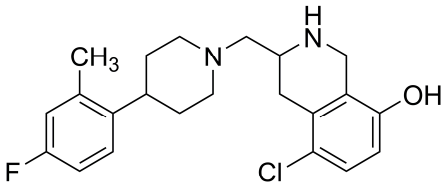

Highly potent and highly selective human NOP receptor antagonist

Running title: Design, synthesis, and SAR studies of nonpeptide NOP receptor antagonists

Discovery of small-molecule nonpeptide antagonists of nociceptin/orphanin FQ receptor: The studies of design, synthesis, and structure–activity relationships for (4-arylpiperidine substituted-methyl)-[bicyclic (hetero)cycloalkanobenzene] derivatives

Shigeo Hayashi*, Katsuyo Ohashi, Sachiko Mihara, Eriko Nakata, Chie Emoto, Atsuko Ohta

Pfizer Global Research & Development, Nagoya Laboratories, Pfizer Japan Inc., 5-2 Taketoyo, Aichi 470-2393, Japan

* Corresponding author. *E-mail address:* Shigeo_Hayashi@nifty.com

Abstract

Nociceptin/orphanin FQ (N/OFQ) and N/OFQ peptide (NOP) receptor are expressed and distributed in various regions such as central nervous system (CNS), peripheral nervous system, immune system, and peripheral tissues. N/OFQ and NOP receptor have important roles on a variety of physiological, pathophysiological, regulatory, and dysregulatory mechanisms in the living body. Both activation and blockade of NOP receptor function have displayed clinical potential of NOP receptor agonists and

antagonists for the treatment of various diseases or pathophysiological conditions, respectively. Potent and selective NOP receptor agonists/antagonists are also useful tools to investigate the various mechanisms mediated by NOP receptor–N/OFQ system. As the present study, a series of (4-arylpiperidine substituted-methyl)-[bicyclic (hetero)cycloalkanobenzene] analogs was designed, synthesized, and biologically evaluated *in vitro* to seek and identify potent and selective, small-molecules of nonpeptide NOP receptor antagonists, which resulted in the discovery of novel potent small-molecule **15** with high human NOP receptor selectivity over human μ receptor. The structure–activity relationship (SAR) of the potency and selectivity, structure–metabolic stability relationship (SMR), and SAR of hERG (human *ether-a-go-go* related gene) potassium ion channel binding affinity for the analogs in the present studies *in vitro* provided or suggested significant and/or useful structural determinants and insights for the respective purposes. The superior profiles of compound **15** are discussed with a viewpoint of multisite interactions between ligand and NOP receptor, together with the results of previous NOP receptor agonist/antagonist studies.

Keywords Nociceptin/Orphanin FQ (N/OFQ) · Human NOP (ORL1) receptor selective antagonist · Multisite interactions with NOP receptor · Metabolic stability · HERG potassium ion channel binding · Prolong QT interval issues.

Abbreviations: GPCR, G-protein-coupled receptor; N/OFQ, nociceptin/orphanin FQ; NOP receptor, N/OFQ peptide receptor [or opioid-receptor-like-1 (ORL1) receptor]; hNOP receptor, human NOP receptor; [^{35}S]GTPγS, [^{35}S]guanosine 5′-(γ-thiotriphosphate); SAR, structure–activity relationship; SMR, structure–metabolic stability relationship; HPCOM, {1-[4-(2-{hexahydropyrrolo[3,4-*c*]pyrrol-2(1*H*)-yl}-1*H*-benzimidazol-1-yl)piperidin-1-yl]cyclooctyl}methanol; MCOPPB, 1-[1-(1-methylcyclooctyl)-4-piperidinyl]-2-[(3*R*)-3-piperidinyl]-1*H*-benzimidazole; HEK, human embryonic kidney; CHO, Chinese hamster ovary; HLM, human liver microsome; hERG, human *ether-a-go-go* related gene; WSCI, water soluble carbodiimide, that is, 1-ethyl-3-(3-dimethylaminopropyl)carbodiimide hydrochloride; HOBT, 1-hydroxybenzotriazole; LAH, lithium aluminum hydride; HBD, hydrogen bond donor.

1. Introduction

Nociceptin [1a]/orphanin FQ [1b] (N/OFQ), that is a metabolite of precursor polypeptide (prepro-N/OFQ), has seventeen amino acid sequence. N/OFQ is an endogenous ligand of N/OFQ peptide (NOP) receptor [or opioid-receptor-like-1 (ORL1) receptor]. NOP receptor has seven transmembrane domains in its structures, and belongs to heterotrimeric GTP-binding protein (G-protein)-coupled receptors (GPCRs) [1c–e]. N/OFQ and NOP receptor are widely expressed and distributed, especially, in the central nervous system (CNS), peripheral nervous system (PNS), immune system, and peripheral tissues, such as brain, spinal cord, peripheral sensory ganglia neurons, lymphocytes, monocytes, and smooth muscles. NOP receptor activation by N/OFQ induces (i) inhibition of cyclic adenosine-3′,5′-monophosphate (cAMP) accumulation and of Ca^{2+} channel currents, (ii) enhance of K^{+} channel currents, (iii) regulation or attenuation of concentration levels of various signal messengers or neurotransmitters such as tachykinins, noradrenaline, 5-hydroxytriptamine, dopamine, and proinflammatory cytokines, (iv) suppression of excitatory synaptic transmissions of neurons, (v) activation of mitogen-activated protein kinases (MAPKs) and of nuclear factor κB (NFκB), and (vi) modulation of immune functions and of transcriptional activations. The biological responses are dependent on the regions, sites, tissues, systems, and physiological conditions, respectively. Hence, NOP receptor–N/OFQ system has key roles in a variety of physiological signal-transduction pathways and behavioral functions in the living body [1a–e,2a–g] (for detailed roles of NOP receptor–N/OFQ system, see also refs. [3–7] and cited references therein). Notably, the expression/distribution levels of (i) NOP receptor, its messenger RNA (mRNA), and splice variants of the receptor, and of (ii) prepro-N/OFQ, N/OFQ, and other metabolites of prepro-N/OFQ are widely varied dependent on (patho)physiological or disease conditions, and are dependent on the regions, sites, tissues, and systems of the body in animal models or in humans [2c,8l–o]. Furthermore, N/OFQ is metabolically converted into inactive or variously-bioactive shorter-fragments by (i) the corresponding processing-enzymes such as peptidases or (ii) further processing/truncation, dependent on the regions/sites/tissues of the body [2a,3,5,9–14] (see also further discussion in refs. [3,5]).

Significantly, both activation and inhibition of NOP receptor function have displayed clinical potential of NOP receptor agonists and antagonists, respectively [2a,b,e]. Thus, utilization of NOP receptor activation is an attractive target for the treatment of neuropathic pain, anxiety disorders, and other diseases (see refs. [3–5] and cited references therein). Blockade against N/OFQ-induced biological function of NOP receptor is an attractive target for the treatment of depressive disorders [15], hyperphagia or hyperphagic obesity [16,17], and hypotension [18]. NOP receptor is distinct from the receptors of classical opioid peptides, although the receptors share high structural and genetic-coding similarities. NOP receptor–N/OFQ binding stimulated-[^{35}S]guanosine 5′-(γ-thiotriphosphate) ([^{35}S]GTPγS) binding response in the spinal cord of rodents was not affected by antagonists of classical opioid receptors or of other various GPCRs; but the [^{35}S]GTPγS binding response was inhibited by a NOP receptor antagonist [19a]. The N/OFQ induced-inhibition of cAMP accumulation was not affected by classical opioid receptor antagonists or agonists *in vitro* [1b]. Besides, classical opioid drugs have been broadly prescribed with careful restriction or control in the medical practices, owing to classical opioid receptor-derived serious adverse effects, such as respiratory restriction and sedation [19b–d]. Therefore, in drug-discovery studies of NOP receptor agonists/antagonists toward clinical drugs, the assessments of their NOP receptor selectivities are very important, especially against μ receptor [or μ-opioid peptide (MOP) receptor], to avoid the adverse effects.

Taken together, potent, selective, and metabolically stable NOP receptor agonists and antagonists are important to investigate their (potential) clinical utilities. The compounds are also useful tools to scrutinize a variety of (patho)physiological, regulatory, and disease mechanisms mediated by the receptor and metabolically unstable N/OFQ, with confirming/verifying intrinsic activity of the endogenous ligand in the mechanisms. In fact, design, synthesis, structure–activity relationship (SAR) and structure―metabolic stability relationship (SMR) of distinctive nonpeptide NOP receptor agonists and antagonists have been investigated, respectively, by Hayashi et al. [3–7]. The agonist studies resulted in the discovery of NOP receptor full agonists, {1-[4-(2-{hexahydropyrrolo[3,4-*c*]pyrrol-2(1*H*)-yl}-1*H*-benzimidazol-1-yl)piperidin-1-yl]cyclooctyl}methanol (HPCOM) as a peripheral and/or spinal

cord-selective, systemically potent analgesic for the treatment of neuropathic pain [3] and 1-[1-(1-methylcyclooctyl)-4-piperidinyl]-2-[(3*R*)-3-piperidinyl]-1*H*-benzimidazole (MCOPPB) as a brain selective, orally potent anxiolytic [4,5], with respective unique and significant profiles *in vitro* and *in vivo*. The antagonist studies resulted in the discovery of several significant and characteristic NOP receptor antagonists *in vitro* [6,7]. Alternatively, various types of chemical entities of NOP receptor antagonists are useful or helpful to explore further opportunity/potentiality. Moreover, different or new types of ligands might be helpful to light on different or new aspects of interaction mechanisms between NOP receptor and agonists/antagonists. Particularly, small-size ligands might be useful tools to search for functionally/transductionally indispensable interaction point/region/residue of NOP receptor protein [7].

Hence, we explored small molecules of further chemotypes that were distinctive from the analogs of the previous reports. Thus, design, synthesis, SAR, and SMR of a series of (4-arylpiperidine substituted-methyl)-[bicyclic (hetero)cycloalkanobenzene] analogs were investigated *in vitro* in order to seek and identify potent, selective, and metabolically stable, novel nonpeptide NOP receptor antagonists. Design and SAR of the analogs for reducing hERG (human *ether-a-go-go* related gene) potassium ion channel binding affinity were also investigated *in vitro* as a safe-drug study. Through the studies, key or significant factors and molecular bases for getting or improving desired characteristics of the analogs were investigated in fundamental and practical viewpoints for the present and further studies. Herein, the unique and significant results and findings are described and discussed, together with the results of the previous NOP receptor antagonist and agonist studies.

2. Results and Discussion

2.1. Chemistry

Various types of (4-arylpiperidine substituted-methyl)-[bicyclic (hetero)cycloalkanobenzene] analogs were prepared for the present design, SAR, and SMR studies.

First, as depicted in Scheme 1, tetrahydroisoquinoline **5** was synthesized. Thus, 4-(4-fluoro-2-methylphenyl)piperidine **1** was prepared [6] then reacted with 2-(*tert*-butoxycarbonyl)-1,2,3,4-tetrahydroisoquinoline-3-carboxylic acid **2** [4,20]. The *N*-Boc portion of the resulting amide **3** was deprotected by acidic condition to afford compound **4**. The carboxamide was subsequently reduced with lithium aluminum hydride (LAH) [7] to afford the desired product **5**, exclusively.

As depicted in Scheme 2, 5-chloro-tetrahydroisoquinolin-8-ol **15** was synthesized. Thus, diethyl acetamidomalonate **6** and *O*-silylated 3-(bromomethyl)-4-chlorophenol **7** [21] were coupled using NaH to afford compound **8** followed by treatment of concentrated HCl in acetic acid to give 2-chloro-5-hydroxyphenylalanine **9**. Pictet–Spengler tetrahydroisoquinoline synthesis was then performed with formaldehyde to afford compound **10** [22]. The secondary-amine was *N*-Boc protected to afford compound **11**. The product was contained a by-product **12** that would plausibly be *N,O*-di-Boc derivative of compound **11**, that is, 2-(*tert*-butoxycarbonyl)-8-(*tert*-butoxycarbonyloxy)-5-chloro-1,2,3,4-tetrahydroisoquinoline-3-carboxylic acid. Finally, compounds **1** and **11** were exclusively transformed into the requisite product by sequential reactions, that is, amidation to afford compound **13**, *N*-deprotection to afford compound **14**, and borane reduction to afford compound **15**.

Other tetrahydroisoquinolines **18** and **19** were prepared in a similar manner for the above synthesis of compounds **4** and **5**, respectively. Thus, after spiro[indane-1,4′-piperidine] **16** and compound **2** were coupled, the resulting compound **17** was *N*-deprotected by acidic condition to afford compound **18**. The carboxamide was reduced with LAH to afford compound **19**. Modifications around cycloamino moiety within the tetrahydroisoquinoline skeleton of compound **19** were also carried out. Thus, *N*-Me derivative **20** was synthesized from compound **17** by simultaneous LAH reductions of the *N*-Boc portion [4] and of the linker carbonyl portion. *N*-Me-1-oxo derivative **21** was synthesized by $KMnO_4$ oxidation [23] of compound **20**. *N*-Ac derivative **22** was synthesized by acetylation of compound **19** (Scheme 3). Furthermore, various modifications on the phenyl moiety within the tetrahydroisoquinoline skeleton

were performed. 5-Chloro-8-hydroxy derivative **23** was prepared from compounds **16** and **11** by way of amidation, *N*-deprotection, and borane reduction in the same way for the above synthesis of compound **15** (Scheme 4). Using the same manner, 5-bromo-8-hydroxy derivative **25** was obtained from the corresponding 5-bromo-8-hydroxy-1,2,3,4-tetrahydroisoquinoline-3-carboxylic acid **24** [22] (Scheme 4). 5-Bromo-8-hydroxy derivative **25** was *N*-Boc protected to prevent low conversion in the following reaction; then hydrogenolysis of the 5-bromo group was performed similar to a synthesis of a *N*-Boc des-bromo-tetrahydroisoquinoline derivative [22]. The resulting compound **26** was *N*-deprotected to afford 8-hydroxy derivative **27**. *N*-Boc compound **29**, that was prepared from 6-hydroxy-1,2,3,4-tetrahydroisoquinoline-3-carboxylic acid **28** [24], was converted into the corresponding 6-hydroxy derivative **30** in the same way for the synthesis of compound **15** (Scheme 5).

On the other hand, chromane **33** was prepared from compound **16** and chromane-3-carboxylic acid **31** in a similar manner for the synthesis of compound **5** (Scheme 6). Tetrahydronaphthalene **38** was prepared from compound **16** and 1,2,3,4-tetrahydronaphthalene-2-carboxylic acid **37** in high-speed parallel synthesis of 1′-(substituted methyl)-spiro[indane-1,4′-piperidine] derivatives **36**. As the synthesis, compound **16** was coupled with carboxylic acids **34** by way of carboxylic acid activation using polymer supported carbodiimide. The resulting amides **35** were reduced with LAH to afford compounds **36** (Scheme 7, further data not shown).

2.2. Design and SAR studies of NOP receptor antagonists *in vitro*

The design, synthesis, and SAR of the present (4-arylpiperidine substituted-methyl)-[bicyclic (hetero)cycloalkanobenzene] analogs were investigated *in vitro* in order to seek and identify potent and selective, novel small molecules of human NOP (hNOP) receptor antagonists, which was the primary purpose of this study. Notably, the design study was also performed with pharmacokinetic study *in vitro* and hERG binding study *in vitro* for the analogs in multiviewpoint strategies (see later sections). The *in vitro* biological assays were performed with the described methods in the previous reports [6,7,25].

Briefly, the binding affinities (K_i values) of the synthetic analogs to hNOP receptor were measured by displacement of tritium-labeled N/OFQ for the recombinant hNOP receptor expressed in human embryonic kidney (HEK)-293 cells. For the evaluation of the *in vitro* binding selectivities for NOP receptor over μ receptor, the binding affinities of the analogs to human μ receptor expressed in Chinese hamster ovary (CHO)-K1 cells were measured by displacement of radiolabeled ligand, [^{3}H]DAMGO. The hNOP receptor antagonist activities of the analogs were evaluated as inhibitory activities against functional activity of hNOP receptor in response to N/OFQ binding. Thus, the activities (IC_{50} values) were determined against [^{35}S]GTPγS binding to α-unit of G-protein stimulated by hNOP receptor–N/OFQ binding in HEK-293 cells. The *in vitro* SAR of the analogs is summarized in Table 1.

In the previous studies [6,7], effective structural units to get potent and selective hNOP receptor antagonists were designed, and the respective significant features were illustrated in Scheme 8. For example, 4-(4-fluoro-2-methylphenyl)piperidine unit was established as a preferable β-substituent portion of 1-(β-amino substituted-β-alanyl)-*N*,*N*-dimethylindoline-2-carboxamide analogs for potency and selectivity; especially attributed to the 4-fluoro and 2-methyl substituents of the unit for compound **39** (1-{3-[4-(4-fluoro-2-methylphenyl)piperidin-1-yl]propanoyl}-*N*,*N*-dimethylindoline-2-carboxamide) [6]. As another structural feature of the compound, two amido-portions and one bicyclo-portion of the *N*,*N*-dimethylindoline-2-carboxamide unit restrict the changes of conformation/orientation of the portions, whereas the whole structure of the molecule is some-extent large and intricate. By contrast, compounds **40**, thus, 1-(aza-alicyclic or carbo-alicyclic group substituted-propyl)-4-arylpiperidine analogs have smaller and simpler structures than compound **39**; and effectiveness of the monocyclic unit at C-3 position of the three-methylene linker on the arylpiperidine unit for potency and selectivity were displayed in comparison with various 1-(3′-substituted propyl)-4-arylpiperidine derivatives [7]. As an imaginary ring-closure way that is illustrated for compound **39′**, one methylene can be inserted between C-2 position of the linker portion on the piperidine ring and *ortho*-position of the phenyl ring. In this case, it is interesting that the nitrogen atom of the piperidine ring and the *ortho*-carbon atom of the

phenyl ring are connected with four single-bonds, similar to the four single-bonds of the linker portion between the piperidine ring and the monocyclic unit of compounds **40**. On the basis of the above results and consideration, (i) combination of 4-(4-fluoro-2-methylphenyl)piperidine unit and cyclic unit by connecting with four single-bonds and (ii) restriction of location/orientation of the cyclic unit by ring closure between the unit and the linker portion, such as a tetrahydroisoquinoline ring, were expected to be a promising or attractive design concept of potent and selective, small-molecules of NOP receptor antagonists. In fact, newly designed compounds **41**, that is, 3-{[4-(4-fluoro-2-methylphenyl)piperidin-1-yl]methyl}-tetrahydroisoquinoline analogs exhibited superior characteristics as small molecules. Tetrahydroisoquinoline analog **5** and 5-chloro-tetrahydroisoquinolin-8-ol analog **15** demonstrated potent hNOP receptor binding affinities (K_i = 3.56 nM and 3.03 nM), high hNOP receptor binding selectivities against human μ receptor (96.1-fold and greater than 143-fold), and potent hNOP receptor antagonist activities (IC_{50} = 58.8 nM and 28.7 nM), respectively. Significantly, compared with 4-arylpiperidine portion of tetrahydroisoquinoline analogs, the binding selectivities of 4-(4-fluoro-2-methylphenyl)piperidine analogs **5** and **15** were much higher than that of the corresponding spiro[indane-1,4′-piperidine] analogs **19** and **23**, respectively. Notably, in comparison with unsubstituted tetrahydroisoquinoline analogs, compound **19** exhibited 3.63-fold drop in binding selectivity and 4.22-fold decrease in antagonist activity than that of compound **5**, respectively.

With respect to the linkage part between 4-arylpiperidine portion and tetrahydroisoquinoline portion, replacement of the methylene linker of compound **19** by carbonyl group, thus, amide analog **18**, led to loss of binding affinity (see later discussion).

SAR study of benzo-fused bicyclo portion using spiro[indane-1,4′-piperidine] template gave further significant results.

Modifications on nitrogen atom of tetrahydroisoquinoline ring, even by small group, led to less potent binding affinities and lower binding selectivities relative to compound **19**. The rank of the orders of binding affinities and binding selectivities was related to the size/volume of this portion, thus *NH* analog **19** > *N*-Me analog **20** > *N*-Ac analog **22**, respectively. *N*-Me-1-oxo (lactam) analog **21** lost hNOP

receptor binding affinity and retained weak human μ receptor binding affinity. *N*-Acetamide analog of compound **19**, that is, 2-[3-{(spiro[indane-1,4′-piperidin]-1′-yl)methyl}-3,4-dihydroisoquinolin-2(1*H*)-yl]acetamide (not shown), led to inferior profiles as well, that is, K_i = 18.1 nM for hNOP receptor, K_i = 108 nM for human μ receptor, and 5.97-fold hNOP receptor binding selectivity against human μ receptor. Substituent effects on the aryl moiety within the bicyclo portion, with the various modification patterns (functional group, position, and/or number of substituent), highly influenced antagonist profiles. For example, relative to compound **23**, tetrahydroisoquinolin-8-ol analog **27** showed comparative binding affinity and higher binding selectivity, but less potent antagonist activity. Exchanging 8-hydroxy group (**27**) by 6-hydroxy group (**30**) gave much less potent binding affinity, higher binding selectivity, and much less antagonist activity, which indicated regioselective effects of phenolic hydroxy group for the profiles.

Furthermore, replacement of the azacyclic moiety within the tetrahydroisoquinoline ring by other (hetero) alicyclic moiety was investigated to explore SAR. Exchanging by oxacyclic moiety, chromane analog **33** exhibited potent binding affinity (K_i = 5.65 nM) with potent antagonist activity as an unsubstituted bicyclic analog, although its binding selectivity was reduced relative to tetrahydroisoquinoline analog **19**. Relative to oxacyclic analog **33**, carbocyclic analog **38** showed comparative binding affinity and improved hNOP receptor binding selectivity (52.1-fold), but much reduced antagonist activity (IC_{50} = 683 nM).

As presented in the SAR studies around (hetero) alicyclic moiety including the modifications around azacyclic moiety of tetrahydroisoquinoline ring such as compounds **19**–**22**, the characters of the moiety, that is, atom species, functional group, basicity, steric hindrance, and modification pattern/mode, are crucial for increasing or decreasing of binding affinities, binding selectivities, and antagonist activities. In the previous study for comparison of substitutions on 1′-propyl portion of spiro[indane-1,4′-piperidine] analogs [7] (see also compounds **40**, Scheme 8), 1′-(3-phenylpropyl)-spiro[indane-1,4′-piperidine] was a poor analog relative to 1′-[3-(unsubstituted aza-alicyclic or carbo-alicyclic group) substituted-propyl]-spiro[indane-1,4′-piperidine] analogs. Significantly, the profiles of the 3-

phenylpropyl analog were also inferior to that of the present tetrahydroisoquinoline analog **19**, chromane analog **33**, and tetrahydronaphthalene analog **38** that have the same spiro[indane-1,4′-piperidine] unit. Indeed, the 3-phenylpropyl analog showed low hNOP receptor binding affinity (K_i = 23.0 nM), low hNOP receptor selectivity against human μ receptor (3.0-fold), and very weak hNOP receptor antagonist activity (IC_{50} = 2,087 nM). The preference of the bicyclic analogs over the 3-phenylpropyl analog would be due to or contributed by restriction/rigidity effect of the location and orientation for the aryl moiety as a part of bicyclo portion, and/or size/volume effect of the (hetero) alicyclic moiety.

As an additional exploratory study of the bicyclo portion, 1′-[benzo-fused (hetero) aryl]methyl-spiro[indane-1,4′-piperidine] derivatives were investigated. As a result, the inhibitory activities of the analogs to hNOP receptor at 100 nM were 56% for 1′-(quinolin-3-ylmethyl) analog, 13% for 1′-[(naphthalen-2-yl)methyl] analog, 66% for 1′-[(1*H*-indol-3-yl)methyl] analog, and 9% for 1′-[(benzofuran-2-yl)methyl] analog, respectively (further data not shown). Their weak or very weak hNOP receptor binding affinities would indicate disadvantage of high π-electron densities of their (hetero) aryl moieties relative to the benzo-fused (hetero) alicyclic analogs.

It is significant to consider molecular bases for distinct pharmacological activities between agonists and antagonists of NOP receptor.

In the previous *in vitro* SAR studies, (i) there were first-order correlations of the levels of functional activities (EC_{50} values for [^{35}S]GTPγS binding-induction) to that of respective binding affinities (K_i values) for hNOP receptor full agonists, MCOPPB and its derivatives; whereas MCOPPB showed more potent efficacy than N/OFQ, thus, E_{max} (efficacy) value of MCOPPB was 140% of maximal response of N/OFQ [4]. (ii) There were first-order correlations of the levels of inhibitory activities (IC_{50} values) against N/OFQ-stimulated [^{35}S]GTPγS binding to that of respective binding affinities (K_i values) for hNOP receptor antagonists, compound **39** and its derivatives, or representative derivatives of compounds **40**, respectively [6,7]. Consequently, it was indicated that the respective primary mechanisms of (i) the G-protein activation responses by the agonists and of (ii) the inhibitions by the

antagonists against the N/OFQ-induced biological response are due to the bindings of the respective ligands to NOP receptor. The distinctive biological responses, that is, activation and inhibition *via* NOP receptor binding of the respective ligands come from their differential interaction-patterns/-modes owing to the respective whole and local structural features of the ligands. Indeed, through the present and previous studies of potent and selective NOP receptor agonists/antagonists [3,4,6,7], their structural features of size, shape, and conformational flexibility/rigidity, functional group, and electronic character have been crucial for their binding affinities, selectivities, and biological activities, respectively.

As studies for the endogenous ligand, it has been reported that the binding regions of NOP receptor protein for N/OFQ are in the second extracellular loop domain [26–29] and in the transmembrane domain [26,30,31]. The binding site in the transmembrane domain works for NOP receptor activation by N/OFQ, which are affected by mutation of amino acid residues of the protein. For example, Asp110, Gln107, Asp130, Tyr131, Gln280, Asn133, and Gln286 were functionally indispensable to exhibit N/OFQ binding induced-biological response of the receptor [30–32]. As well, replacement studies for amino acid residues of N/OFQ have revealed various sites of the heptadecapeptide are required for both binding and activation of NOP receptor or either of them. For example, the residues located at positions 1–8, 12, 14, and 17 were important for the receptor activation [33,34]. Besides, it was strongly suggested that binding mode of a peptide NOP receptor antagonist was different from that of N/OFQ; and the binding site for the antagonist would be shared in part but not be shared in the other part of the binding site for N/OFQ [29].

The requirements of the effective multisite-interactions between N/OFQ and NOP receptor in orthosteric binding site for potent and selective binding and function are in line with the facts that potent and selective, binding affinities and functional activities of synthetic NOP receptor agonists such as HPCOM and MCOPPB were derived from their multisite characteristic portions as described in the SAR studies [3,4]. On the contrary, to block N/OFQ-induced signal transduction of NOP receptor, distinctive structural features of NOP receptor antagonists are significant in the orthosteric binding site

in order to physically or functionally mask or interfere with the crucial points/regions involved in the activation of the protein.

For elucidating or understanding detailed molecular mechanisms, the effective or crucial structural determinants of potencies, selectivities, and activities for the present analogs would be important. Particularly, the SAR of the present small molecules shows various triggers to set off the antagonism, including some discrepancies for potency relationships between the binding affinities and the antagonist activities dependent on their structures. Indeed, (i) relative to the potent antagonist activity of 4-(4-fluoro-2-methylphenyl)piperidine analog **5**, the activity of the corresponding spiro[indane-1,4′-piperidine] analog **19** was much decreased. By conversion of its tetrahydroisoquinoline portion into other benzo-fused (hetero) alicyclic portions, the less antagonist activity of compound **19** was some-degree improved but not enough to reach the level of compound **5** in the case of compound **33**, and rather weakened in the case of compound **38**, although the binding potencies were some-degree improved in the both cases. These results indicated strong contribution of the character of 4-(4-fluoro-2-methylphenyl)piperidine as 4-arylpiperidine portion for the potent antagonist activity of compound **5**. (ii) Compared with compound **5** (or compound **19**), compound **15** (or compound **23**) exhibited much increased antagonist activity, relative to the change of binding affinities between them, indicating strong contribution of chloro group and hydroxy group, that are appropriately located on the aryl moiety of tetrahydroisoquinoline portion, for the activity. (iii) The presence/absence and the nature of (hetero) alicyclic moiety within the bicyclo portion can be geared to evoke or lose antagonist activity, in addition to the restriction/rigidity effect of location and orientation for the aryl ring moiety within bicyclo portion as mentioned. As supporting SAR information of other synthetic NOP receptor antagonists in the previous studies (see also Scheme 8), (i) the binding affinities and the antagonist activities of the derivatives of *N*,*N*-dimethylindoline-2-carboxamide analog **39** were dependent on various structural features of respective 4-phenylpiperidine portions [6]. (ii) The affinities and the activities of the 4-arylpiperidine analogs **40** were dependent on various structural features of respective cyclic groups at propyl portion [7]. (iii) Discrepancies between the potencies of binding affinities and antagonist

activities have been found for some types of compounds. The discrepancies in the present and the previous studies might be dependent on whether the ligand binding-induced physically or functionally masking or interfering with functionally important points/regions of the receptor protein were effectual or not [6,7].

Recently, an independent study with X-ray crystallography for complex of NOP receptor and an antagonist C-24 (1-benzyl-*N*-{3-[spiroisobenzofuran-1(3*H*),4′-piperidin-1-yl]propyl}pyrrolidine-2-carboxamide) was reported [32]. In the study, the binding site of the ligand was deep within seven-transmembrane helical core of the receptor; the spiro[isobenzofuran-1,4′-piperidine] portion was buried in a hydrophobic cavity; and the isobenzofuran group was interposed between Met134 and Tyr131. Furthermore, the protonated nitrogen of piperidine ring of the ligand formed a salt bridge with Asp130 that is an important point required for both N/OFQ and NOP receptor antagonists [32]. The present antagonists, compounds **5** and **15** (as well as compounds **19** and **23**) might share similar orthosteric binding sites in the transmembrane core owing to some structural similarities of the arylpiperidine portions between the present compounds and the ligand, although the other portions are quite different. Assuming that the arylpiperidine portions as respective scaffolds for the present analogs and the ligand bind at almost the same site within the binding pocket and have similar interaction modes (location and orientation), one of pharmacophore profiles of the present analogs might also be explicable. Thus, the protonatable nitrogen of the piperidine ring of the respective present analogs might work for anchoring salt bridge with Asp130 as a critical interaction, similar to the above manner. Notably, compound **18** that is amide analog of the pyridine ring did not show the binding affinity, which might explain indispensability of the protonatable amino-moiety of the present analogs for their interactions with the receptor protein, as well.

Taken together, as significant findings of the present studies, (i) the newly designed compound **15** was discovered as a novel small-molecule nonpeptide hNOP receptor antagonist that demonstrated highly potent hNOP receptor binding affinity, high hNOP receptor binding selectivity against human μ receptor, and highly potent hNOP receptor antagonist activity *in vitro*. (ii) The whole and multisite structural or

chemical characters such as size, shape, volume, flexibility/rigidity, atom species, functional group, and electronic state of the present small-molecule analogs were significant or crucial to determine their profiles *in vitro*, which would be associated with the multisite interactions of the ligands to the receptor. Especially, the characteristic portions were indispensable for compound **15** to be a superior small-molecule hNOP receptor antagonist, respectively. The significant results, information, and the present analogs *per se* would be useful to conduct further NOP receptor antagonist studies and might be helpful to elucidate dynamic mechanisms of a variety of biological effects mediated by NOP receptor–ligand system, together with the results and the significant analogs *per se* of the previous studies for the distinctive series of hNOP receptor agonists [3–5] and antagonists [6,7].

2.3. Design and SMR studies of metabolic stability *in vitro*

Alternatively, the design and SMR of the present analogs were investigated as a pharmacokinetic study *in vitro*. The half-lives of the compounds were evaluated in human liver microsome (HLM). The *in vitro* SMR of the analogs is shown in Table 2.

Significantly, the above 4-(4-fluoro-2-methylphenyl)piperidine unit was designed in the previous detailed SAR and SMR investigations with multiviewpoint and integrated drug-design strategy for *N*,*N*-dimethylindoline-2-carboxamide analogs [6], expecting to get compatibility of potent and selective hNOP receptor antagonist activity and metabolic stability. Owing to a successful result in the study, the unit was also thought to be effectual for the present study. Indeed, 4-(4-fluoro-2-methylphenyl)piperidine analogs of the tetrahydroisoquinoline derivatives were investigated. As a significant result, 5-chloro-tetrahydroisoquinolin-8-ol analog **15** was more metabolically stable (21.6 min) than tetrahydroisoquinoline analog **5**. When the arylpiperidine portion was substituted by spiro[indane-1,4′-piperidine], 5-chloro-tetrahydroisoquinolin-8-ol **23** was also more stable than the corresponding tetrahydroisoquinoline analog **19**. As well, SMR study around tetrahydroisoquinoline portion of 1′-[(tetrahydroisoquinolin-3-yl)methyl]-spiro[indane-1,4′-piperidine] analogs was investigated.

Relative to 5-chloro-tetrahydroisoquinolin-8-ol analog **23**, tetrahydroisoquinolin-8-ol analog **27** and tetrahydroisoquinolin-6-ol analog **30** exhibited comparative stabilities. 5-Bromo-tetrahydroisoquinolin-8-ol analog **25** showed shorter half-life than that of compound **23**. Generally, phenolic analogs **15**, **23**, **25**, **27**, and **30** were more metabolically stable compared to the corresponding unsubstituted analogs **5** and **19**. Besides, chromane analog **33** was less stable than tetrahydroisoquinoline analog **19**. As supporting data for the above SMR of 1′-(substituted alkyl) portion of spiro[indane-1,4′-piperidine] analogs, compound **19** was more stable than 1′-(3-phenylpropyl)-spiro[indane-1,4′-piperidine] (3.0 min) of which the monocyclic phenyl portion was very weak against metabolic reaction in HLM as described in the previous study [7].

It is significant to consider contributing-factor or -effect for enhancing/improving metabolic stability in the viewpoint of structural features or chemical properties, with the results of the previous SMR studies for a variety of compounds in HLM [3,5–7]. First, in the previous studies, the structural differences of the 4-arylpiperidine portions influenced respective stabilities of compounds. As reported, 4-(4-fluoro-2-methylphenyl)piperidine was much preferable to 4-(2-methylphenyl)piperidine as 4-arylpiperidine portion of *N*,*N*-dimethylindoline-2-carboxamide analogs; and the 4-fluoro group effect on the aryl moiety for enhancing stability in the comparison was in accord with SMR of other analogs in the study as well as a result of major-metabolite identification study for a related compound, thus 4-position of its aryl moiety was hydroxylated in liver microsome [6]. In another study, 4-(2-methylphenyl)piperidine was preferable to spiro[indane-1,4′-piperidine] as 4-arylpiperidine portion of (piperidin-1-yl)propyl analogs [7]. The preference of 4-(4-fluoro-2-methylphenyl)piperidine for compound **15** over spiro[indane-1,4′-piperidine] for compound **23** in the present study was in line with the results of those studies, thus the differences of metabolic stabilities between compound **15** and compound **23** were attributable to their 4-arylpiperidine portions as well. Second, as the SMR for the opposite part of 4-arylpiperidine portion of the present compounds, the structural differences of the benzo-fused bicyclic portion variously affected their respective stabilities as described (for example, compound **15** > compound **5**). As substituents on propyl group for 1′-propyl-spiro[indene-1,4′-piperidine] analogs, γ-

hydroxypiperidine and 2-piperidone were much preferable to piperidine, while cyclohexane and benzene were much less favorable over piperidine [7]. These results have indicated that the structural features and/or chemical properties of both 4-arylpiperidine portion and the opposite part would contribute to the overall metabolic stability or lability of the respective compounds. Noteworthy, the respective structural features and/or chemical properties of specific moiety or portion have been more apparently responsible for the differences of metabolic stabilities between analogs in the comparisons on condition that the features and/or the properties of the other moiety or portion of the analogs were similar. Assuming that the unsubstituted tetrahydroisoquinoline portions of compounds **5** and **19** are important sites involved in the metabolically labilities of the compounds, the various results of the SMR study around bicyclo portion of the present analogs might show further potential contributing-factors/-effects in terms of metabolic stabilities of the analogs; although identification study of possible metabolites of compound **5** or its analogs would also be important or helpful to understand them. Thus, more favorable characters of secondary-amino alicyclic group and phenolic group for metabolic stability in comparison of the analogs might be due to or contributed by hydrogen bond donor (HBD) functionality (or reduced local lipophilicity) of them, compared to the corresponding oxacyclic group and des-hydroxy-phenyl group analogs that have no HBD functionality, respectively. Supportingly, HBD functionality effects [or reduced (local) lipophilicity effects attributable to (local) structural differences] for getting/enhancing metabolic stability in HLM can be seen for (i) plasma-to-brain selective HPCOM, that is *NH*-hexahydropyrrolo[3,4-*c*]pyrrole analog of (hydroxymethyl)cyclooctyl-type benzimidazole derivative, against the corresponding *N*-Me-piperazine analog [3], for (ii) brain selective MCOPPB, that is *NH*-piperidine analog of methylcyclooctyl-type benzimidazole derivative, against the corresponding *N*-Me-piperidine analog [5], and for (iii) (β- or γ-)hydroxypiperidine analogs of 1-(3′-substituted propyl)-4-arylpiperidine derivatives against the corresponding unsubstituted piperidine analog [7], respectively. Furthermore, introduction of hydroxy group onto phenyl moiety within tetrahydroisoquinoline portion for the present analogs heightens oxidation-state and acidity of the moiety, which might potentially increase resistivity of the moiety against oxidation by major metabolic enzymes, cytochrome P450s

(CYPs) in HLM. Electron withdrawing characters of both 4-fluoro group of arylpiperidine portion and 5-chloro group of tetrahydroisoquinoline portion of compound **15** would affect π-electron density (distribution) and polarizability of the respective aryl cores, and might affect resistivity against electrophilic oxidative-reaction by CYPs. Besides, appropriately located substituent-effects for metabolic stability in this study might also be associated with their blocking effects against potential metabolic reactions on the respective sites/portions, similar to the potential blocking effect produced by additional substituent for the arylpiperidine analogs in the previous study [6].

In conclusion, (i) compound **15** was most preferable among the present analogs in the viewpoint of the compatibility of metabolic stability in HLM and profiles as highly potent and highly selective hNOP receptor antagonist *in vitro*. (ii) The results of this study suggested significant or potential contributing-factors/-effects for enhancing/improving metabolic stability in comparison of the present analogs, which might be beneficial or helpful to conduct further or other drug-discovery studies of metabolically stable drugs.

2.4. Design and SAR studies of hERG ion channel binding *in vitro* for drug safety

The bindings of (candidate) clinical drugs to hERG potassium ion channel are serious concerns in the pharmacotherapies. The concerns relate to prolongation of QT interval in the electrocardiogram *in vivo*, which may lead to Torsades de Pointes in the human heart or sudden death at worst. Therefore, the assessments of the binding affinities to the channel for drugs are very important in drug-discovery strategies toward clinical medications. Indeed, various types of compounds such as HPCOM [3], MCOPPB [5], and other compounds [7], that have little potential risks of the hERG potassium ion channel binding issues, have been discovered in the respective safe-drug studies.

As well, the design and SAR of the present analogs for reducing hERG potassium ion channel binding affinity were investigated *in vitro*. The inhibitory activities of the analogs (IC_{50} values) were determined

against [^{3}H]dofetilide binding to potassium ion channel from hERG expressed in HEK-293 cells [3,5,7,25]. The *in vitro* SAR of the analogs is shown in Table 2.

In comparison of 4-(4-fluoro-2-methylphenyl)piperidine analogs, 5-chloro-tetrahydroisoquinolin-8-ol analog **15** exhibited less potent binding affinity than tetrahydroisoquinoline analog **5**. Besides, in comparison of spiro[indane-1,4′-piperidine] analogs, tetrahydroisoquinoline analog **19** and 5-halogenated tetrahydroisoquinolin-8-ol analogs **23** and **25** exhibited less potent binding affinities than tetrahydroisoquinolin-6-ol analog **27** and tetrahydroisoquinolin-8-ol analog **30**. Compared with substituent effects on the aryl moiety within tetrahydroisoquinoline portion for spiro[indane-1,4′-piperidine] analogs, the rank of the orders of the binding affinities was 5-chloro-tetrahydroisoquinolin-8-ol **23** < 5-bromo-tetrahydroisoquinolin-8-ol **25** < tetrahydroisoquinolin-8-ol **27** < tetrahydroisoquinolin-6-ol **30**. These results indicated that (i) the orders of the reducing affinity effects of 5-substituents for the respective tetrahydroisoquinolin-8-ol analogs was in accord with the order of the electron negativities of the respective 5-substituents, that is, chloro group (**23**) > bromo group (**25**) > hydrogen group (**27**). By contrast, (ii) phenolic hydroxy groups at 8- or 6-position (**27** or **30**), that have π-electron donating character for the respective aromatic-ring moieties, showed increasing affinity effects compared with hydrogen group (**19**). In addition, the phenolic hydroxy group effects of compounds **27** and **30** displayed regioselectivities for their affinities, that is, 6-OH group (**30**) > 8-OH group (**27**). As supporting data in the previous study *in vitro* in terms of the electron effects, MCOPPB that has *NH*-piperidine (electron-poor ring) as 2-substituent on its benzimidazole moiety showed little hERG ion channel binding affinity, contrary to the corresponding 2-aryl group (electron-rich ring) analogs that showed higher binding affinities [5]. In comparison of (hetero) alicyclic moiety within the bicyclo portion of the present analogs in Table 2, *N*-Me-1-oxo (lactam) analog **21** was very successful to achieve much lower binding affinity (IC_{50} = 6,960 nM); however *N*-Ac analog **22** showed higher affinity. Compared to the other groups for the moiety, the preference of the lactam group for reducing affinity might be associated with its character, that is, electron withdrawing effect of the group for reducing electron density of the adjacent

aryl moiety, electron distribution effect or polarity effect for the hetero alicyclic moiety (that is, lactam group itself) or for the aryl moiety affected by the group, and/or position-dependent steric effect of the amido group, against the ligand binding to the channel. Fuerthermore, local lipophilicity around the (hetero) alicyclic moiety might contribute to the binding affinity. Thus, tetrahydronaphthalene analog **38** that has higher lipophilic carbocyclic moiety showed higher affinity relative to tetrahydroisoquinoline analog **19** that has lower lipophilic secondary-amino alicyclic moiety. The possible lower lipophilicity effect for reducing affinity was in line with previously described lower lipophilicity effects for reducing *in vitro* hERG ion channel binding affinity of (i) 1,2-substituted benzimidazole analogs (for example, MCOPPB that is *NH*-piperidine analog against the corresponding aryl analogs, see also the above discussion) [5] and of (ii) 1-(azacyclic or carbocyclic group substituted-propyl)-4-arylpiperidine analogs (for example, piperidine analog had much less affinity than cyclohexane analog) [7] (for further results of the detailed SAR studies, see the original reports [5,7], respectively). Interestingly, oxacyclic analog **33** was preferable to carbocyclic analog **38** for reducing affinity. The oxacyclic group effect of compound **33** against hERG ion channel binding might be associated with σ-electron withdrawing effect of the ether oxygen atom for reducing electron density of the adjacent aryl moiety, lower lipophilic effect that is similar to the above examples, and/or electron lone-pair effect of the oxygen atom, compared to the carbocyclic moiety of compound **38**.

Overall, i) several structures were found to be effectual for reducing hERG potassium ion channel binding affinity in this study. ii) As significant or potential contributing-factors for reducing affinity, various whole/local structural features and/or chemical properties, such as shape, electron state, polarity, atom species, functional group, and position of substituent/group, were suggested in comparison of the present analogs, which might be associated with interaction levels between the compounds and hERG ion channel. The results and findings might provide useful or helpful information to conduct further or other drug-discovery studies for safe drugs, together with the results of the previous studies for diverse structural types of compounds [3,5,7].

3. Conclusions

In the present study, the design, synthesis, and SAR of a series of (4-arylpiperidine substituted-methyl)-[bicyclic (hetero)cycloalkanobenzene] analogs were investigated *in vitro* in order to seek and identify potent and selective, novel small-molecules of hNOP receptor antagonists. Among them, compounds **5** and **15** were discovered as novel nonpeptide hNOP receptor antagonists that demonstrated highly potent hNOP receptor binding affinities, high hNOP receptor binding selectivities against human μ receptor, and highly potent hNOP receptor antagonist activities *in vitro*. In the design and SMR studies in HLM, compound **15** exhibited more metabolic stability than compound **5**. The SAR and SMR studies indicated or suggested various whole and local features as key and/or useful contributing-factors/-effects to achieve or improve the profiles. In the design and SAR studies of the analogs against hERG ion channel binding affinity *in vitro*, several effective structures and significant and/or useful contributing-factors for reducing affinities were found or suggested. The above results and findings including the significant small-molecule analogs *per se* might provide useful or helpful information/tools to conduct further studies of hNOP receptor antagonists, elucidation studies of NOP receptor–N/OFQ system-mediated pharmacological/functional/transductional mechanisms, and other various studies for metabolically stable and safe drugs.

4. Experimental section

4.1. Chemistry

4.1.1. General procedures

In general, reagents, solvents, and other chemicals were used as purchased without further purification. All reactions with air- or moisture-sensitive reactants and solvents were carried out under nitrogen atmosphere. Flash column chromatography (medium pressure liquid chromatography) purifications were carried out using Merck silica gel 60 (230–400 mesh ASTM). Preparative thin-layer chromatography (PTLC) purifications were carried out on Merck silica gel 60 F_{254} precoated glass plates at a thickness of 0.5 or 1.0 mm. The structures of all isolated compounds were assured by the following techniques, such as NMR, IR, MS or elementary analysis. ^{1}H nuclear magnetic resonance (^{1}H NMR) data were determined at 270 MHz on a JNM-LA 270 (JEOL) spectrometer and at 300 MHz on a JNM-LA300 (JEOL) spectrometer. Chemical shifts are expressed in δ (ppm). ^{1}H NMR chemical shifts were determined relative to tetramethylsilane (TMS) as internal standard. NMR data are reported as follows: chemical shift, number of atoms, multiplicities (s, singlet; d, doublet; t, triplet; dd, double doublet; m, multiplet; and br, broadened), and coupling constants. Infrared spectra were measured by an IR-470 (Shimadzu) infrared spectrometer. Low-resolution mass spectral data (EI) were obtained on an Automass 120 (JEOL) mass spectrometer. Low-resolution mass spectral data (ESI) were obtained on a Quattro II (Micromass) mass spectrometer–Agilent 1100 HPLC system. Melting point was obtained using Exstar 6000 (Seiko Instruments Inc.) and was uncorrected.

After preparation by manual synthesis, compounds **5**, **15**, **18**–**23**, **25**, **27**, **30**, and **33** were converted into salts of citrate, hydrochloride or 4-tosylate, respectively, as shown in the subsections for the compounds, respectively. The purities of citrates of the compounds **5**, **15**, **19**, **23**, **25**, **27**, and **30**, a hydrochloride of compound **22**, and a 4-toluenesulfonate of compound **33** were confirmed by elementary analysis to be within ±0.4% of calculated values, respectively. Elementary analysis of hydrochloride salts of compounds **18**, **20**, and **21** was not performed owing to the requisite amounts for the analysis of the respective salts; however the purity of salt-free compounds **18**, **20**, and **21** were assured by ^{1}H NMR analysis that had no significant impurity signal except small amounts of solvent signals. Compound **38** prepared by high-speed parallel synthesis was obtained as a formate salt. These salts of the compounds were used for pharmacological and/or pharmacokinetic evaluations.

4.1.2. Synthesis of 3-{[4-(4-fluoro-2-methylphenyl)piperidin-1-yl]methyl}-1,2,3,4-tetrahydroisoquinoline (5).

4.1.2.1. *tert*-Butyl 3-{[4-(4-fluoro-2-methylphenyl)piperidin-1-yl]carbonyl}-3,4-dihydroisoquinoline-2(1*H*)-carboxylate (3). To a suspension of 1,2,3,4-tetrahydroisoquinoline-3-carboxylic acid hydrochloride (2.137 g, 10.0 mmol) in H_2O (54.0 mL)–*tert*-butyl alcohol (45.0 mL) was added 2 N NaOH (11.0 mL, 22.0 mmol) at room temperature under N_2. Di-*tert*-butyl dicarbonate (Boc_2O) (2.20 g, 10.1 mmol) was added to the resulting solution at a time, stirred at room temperature under N_2 for 16 h [4,20]. The reaction solution was poured into 10% aqueous citric acid at room temperature, then the resulting acidic mixture was extracted with chloroform three times. The combined extracts were washed with H_2O, dried over anhydrous $MgSO_4$, and concentrated *in vacuo* to afford 3.5196 g of 2-(*tert*-butoxycarbonyl)-1,2,3,4-tetrahydroisoquinoline-3-carboxylic acid **2** [20] as a slight yellowish-white solid (crude).

A mixture of 4-(4-fluoro-2-methylphenyl)piperidine **1** (386.5 mg, 2.00 mmol) [6], 2-(*tert*-butoxycarbonyl)-1,2,3,4-tetrahydroisoquinoline-3-carboxylic acid **2** (554.6 mg, 2.00 mmol), water soluble carbodiimide, that is, 1-ethyl-3-(3-dimethylaminopropyl)carbodiimide hydrochloride (WSCI) (766.8 mg, 4.00 mmol), hydroxybenzotriazole (HOBT) (540.5 mg, 4.00 mmol), and dry Et_3N (836 μL, 6.00 mmol) in dry CH_2Cl_2 (16.0 mL) was stirred at room temperature under N_2 for 24 h [7]. The reaction solution was poured into H_2O (30 mL), and the resulting mixture was extracted with CH_2Cl_2 (30 mL × 2). The combined extracts were dried over anhydrous $MgSO_4$, and concentrated *in vacuo*. The residue was purified by column chromatography (silica gel, hexane/AcOEt = 3:1) to afford 833.5 mg of the title product **3** in 92% yield as a colorless oil. ^{1}H NMR (300 MHz, $CDCl_3$) δ 7.27–7.00 (5H, m), 6.90–6.85 (2H, m), 5.40–4.16 (5H, m), 3.25–2.60 (5H, m), 2.35 (3H, s), 2.00–1.37 (13H, m, including 9H, s, at 1.49 ppm). MS (ESI positive) m/z: $[M+H]^+$ 453.

4.1.2.2. 3-{[4-(4-Fluoro-2-methylphenyl)piperidin-1-yl]carbonyl}-1,2,3,4-tetrahydroisoquinoline (4). A mixture of compound **3** (833.5 mg, 1.84 mmol) in 10% HCl in MeOH (80.0 mL) was stirred at room temperature under N_2 for 40 h, then concentrated *in vacuo*. The residue was partitioned between CH_2Cl_2 (60.0 mL) and saturated aqueous $NaHCO_3$ (100 mL). The organic layer was separted and the aqueous layer was extracted with CH_2Cl_2 (60 mL × 2). The organic layers were combined, dried over anhydrous $MgSO_4$, and concentrated *in vacuo* to afford 603.3 mg of the title product **4** in 93% yield. ^{1}H NMR (300 MHz, $CDCl_3$) δ7.20–7.02 (5H, m), 6.92–6.83 (2H, m), 4.86 (1H, d, J = 12.5 Hz), 4.13 (3H, m), 3.99 (1H, dd, J = 11.0 Hz, J = 4.23 Hz), 3.24–2.66 (5H, m), 2.35 (3H, s), 1.94–1.50 (5H, m). MS (ESI positive) m/z: $[M+H]^+$ 353.

4.1.2.3. 3-{[4-(4-Fluoro-2-methylphenyl)piperidin-1-yl]methyl}-1,2,3,4-tetrahydroisoquinoline (5). To a solution of compound **4** (603.3 mg, 1.71 mmol) in anhydrous THF (15.0 mL) was added lithium aluminum hydride (LAH) (194.9 mg, 5.14 mmol) at 0 °C under N_2 [7]. The reaction mixture was stirred at the temperature under N_2 for 1 h, allowed to room temperature, and stirred under N_2 for 24 h. The reaction mixture was cooled to 0 °C, AcOEt (80 mL) was added dropwise, stirred at the same temperature under N_2 for 20 min, allowed to warm to room temperature, and stirred for 40 min. The mixture was cooled to 0 °C, ice-cooled H_2O (80 mL) was added dropwise, then the resulting mixture was stirred at the temperature for 1.5 h. The organic layer was separated, and the aqueous layer was extracted with AcOEt (80 mL × 2). The organic layers were combined, dried over anhydrous $MgSO_4$, and concentrated *in vacuo*. The residue was purified by column chromatography (silica gel, CH_2Cl_2/MeOH = 14:1), followed by PTLC twice (silica gel, CH_2Cl_2/MeOH = 14:11 for the first, CH_2Cl_2/AcOEt/2-propanol/25% aqueous ammonia = 16:40:4:0.4 for the second) was performed to afford 130.2 mg of the title product **5** in 22% yield. MS (ESI positive) m/z: $[M+H]^+$ 339.24. ^{1}H NMR (300 MHz, $CDCl_3$) δ7.22–7.03 (5H, m), 6.90–6.83 (2H, m), 4.10 (2H, s), 3.15–2.96 (3H, m), 2.76–1.70 (15H, m, including 3H, s, at 2.32 ppm). **Citric acid salt formation, general procedure** [6,7]:

Compound **5** (122.5 mg, 0.362 mmol) and one equivalent of citric acid (69.5 mg, 0.362 mmol) was dissolved in dry CH_2Cl_2 (8.0 mL) and dry MeOH (12.0 mL), and the resulting solution was stirred at room temperature for 2 h, then concentrated *in vacuo*. The residue was resuspended in CH_2Cl_2, collected by filtration, and dried under vacuum at 50 °C for 5 h to afford citrate salt as a white solid. Monocitrate of compound **5:** Mp: 185.7 °C. IR (KBr): 3430, 2932, 1717, 1589, 1499, 1387, 1246, 1188, 972, 864, 820, 752, 613 cm^{-1}. Anal. ($C_{22}H_{27}FN_2 \cdot C_6H_8O_7$) C, H, N.

4.1.3. Synthesis of 5-chloro-3-{[4-(4-fluoro-2-methylphenyl)piperidin-1-yl]methyl}-1,2,3,4-tetrahydroisoquinolin-8-ol (15).

4.1.3.1. Diethyl (acetylamino)(5-{[*tert*-butyl(dimethyl)silyl]oxy}-2-chlorobenzyl)malonate (8). To stirred a solution of diethyl acetamidomalonate (15.9 g, 73.2 mmol) in dry DMF (80.0 mL) was added NaH (60% in oil, 2.92 g, 73.0 mmol) at 0 °C under N_2. The reaction mixture was stirred at room temperature under N_2 for 30 min, then the resulting yellow solution was cooled to 0 °C. A solution of [3-(bromomethyl)-4-chlorophenoxy](*tert*-butyl)dimethylsilane **7**, that was prepared according to the reported method [21] (24.5 g, 73.0 mmol), in dry DMF (20.0 mL) was added to the above solution at 0 °C under N_2. The reaction solution was allowed to warm to room temperature, stirred under N_2 for 2 h, then H_2O (200 mL) was added. The resulting mixture was extracted with AcOEt twice. The combined extracts were washed with H_2O twice and then brine, dried over anhydrous $MgSO_4$, and concentrated *in vacuo*. The residue was purified by column chromatography (silica gel, hexane/AcOEt = 2:1) to afford 18.45 g of the title product **8** as an oil in 54% yield from compound **7**. ^{1}H NMR (300 MHz, $CDCl_3$) δ 7.16 (1H, d, J = 8.6 Hz), 6.66 (1H, dd, J = 8.6 Hz, J = 2.8 Hz), 6.57 (1H, d, J = 2.8 Hz), 6.54 (1H, br s), 4.37–4.07 (4H, m), 3.78 and 3.74 (total 2H, each s), 2.05 and 2.01 (total 3H, each s), 1.29 (6H, t, J = 8.8 Hz), 0.96 (9H, s), 0.17 (6H, s).

4.1.3.2. 2-(*tert*-Butoxycarbonyl)-5-chloro-8-hydroxy-1,2,3,4-tetrahydroisequinoline-3-carboxylic acid (11). A mixture of compound **8** (18.45 g, 39.1 mmol), concentrated HCl (70.0 mL), and acetic acid

(30.0 mL) was warmed to reflux conditions, stirred under N_2 for 14 h, then more concentrated HCl (40 mL) was added. The reaction mixture was stirred under reflux conditions for 10 h, and then more concentrated HCl (10 mL) was added. The reaction mixture was stirred under reflux conditions for 16 h, then cooled to room temperature. The reaction mixture was diluted with H_2O (50 mL), washed with CH_2Cl_2 twice, and then concentrated *in vacuo* to afford 10.2 g of 2-chloro-5-hydroxyphenylalanine hydrochloride **9** as a white solid (crude).

A mixture of compound **9** (10.2 g, crude), 37% formalin (40.0 mL), and H_2O (40.0 mL) was warmed to 90 °C, and stirred under N_2 for 1.5 h, then cooled to 0 °C [22]. The resulting white precipitate was collected by filtration, and dried under vacuum to afford 7.88 g of 5-chloro-8-hydroxy-1,2,3,4-tetrahydroisoquinoline-3-carboxylic acid hydrochloride **10** in 76% yield as a solid. MS (ESI negative) m/z: $[M–H]^-$ 226.02.

To a stirred mixture of compound **10** (7.88 g, 29.8 mmol) and 2 N NaOH (75.0 mL, 150 mmol) in 1,4-dioxane (80.0 mL) was added Boc_2O (7.81 g, 35.8 mmol) at room temperature under N_2. The reaction mixture was stirred at the temperature for 18 h, then concentrated *in vacuo*. The residue was dissolved in H_2O (60.0 mL), then MeOH (30.0 mL) was added followed by 2 N NaOH (20.0 mL). The mixture was stirred at room temperature for 6 h, then concentrated *in vacuo*. The residue was acidified by adding 2 N HCl and 10% aqueous citric acid, and then extracted with CH_2Cl_2–MeOH (10:1) three times. The combined extracts were concentrated *in vacuo* to afford 8.0 g of the title product **11** as a brown solid (crude), containing a by-product **12** that would plausibly be *N*,*O*-di-Boc derivative of compound **11**, that is, 2-(*tert*-butoxycarbonyl)-8-(*tert*-butoxycarbonyloxy)-5-chloro-1,2,3,4-tetrahydroisoquinoline-3-carboxylic acid, as detected by mass spectroscopy: MS (ESI negative) m/z: $[M–H]^-$ 426 (not isolated). Compound **11:** ^{1}H NMR (300 MHz, DMSO-d_6) 10.00 (1H, s), 7.44 and 7.13 (total 1H, each d, J = 8.7 Hz and J = 8.6 Hz), 7.18 and 6.72 (total 1H, each d, J = 8.8 Hz), 5.08–5.00 (0.5H, m), 4.90–4.80 (0.5H, m), 4.50–4.35 (1H, m), 4.30–4.15 (1H, m), 3.50–2.80 (2H, m), 1.50, 1.46, and 1.41 (total 9H, each s). MS (ESI negative) m/z: $[M–H]^-$ 326.

4.1.3.3. *tert*-Butyl 5-chloro-3-{[4-(4-fluoro-2-methylphenyl)piperidin-1-yl]carbonyl}-8-hydroxy-3,4-dihydroisoquinoline-2(1*H*)-carboxylate (13). A mixture of compound **1** (162.3 mg, 0.840 mmol), compound **11** (250.0 mg, crude), WSCI (322.1 mg, 1.68 mmol), HOBT (227.0 mg, 1.68 mmol), and dry Et_3N (351 μL, 2.52 mmol) in dry CH_2Cl_2 (7.0 mL) was stirred at room temperature under N_2 for 36 h, then poured into H_2O (50 mL). The resulting mixture was extracted with CH_2Cl_2 (50 mL × 2). The combined extracts were dried over anhydrous $MgSO_4$, and concentrated *in vacuo*. The residue was purified by column chromatography (silica gel, hexane/AcOEt = 2:1) to afford 218.9 mg of the title product **13** in 52% yield from compound **1**. TLC: R_f =0.35, AcOEt/hexane = 1:1. MS (ESI positive) m/z: $[M+H]^+$ 501.

4.1.3.4. 5-Chloro-3-{[4-(4-fluoro-2-methylphenyl)piperidin-1-yl]carbonyl}-1,2,3,4-tetrahydroisoquinolin-8-ol (14). To a stirred solution of compound **13** (218.9 mg, 0.435 mmol) in anhydrous THF (2.0 mL) was added trifluoroacetic acid (4.0 mL) at 0 °C under N_2. The reaction solution was stirred at the temperature for 1 h, allowed to room temperature, stirred overnight, then concentrated *in vacuo*. The residue was partitioned between CH_2Cl_2 (20 mL) and saturated aqueous $NaHCO_3$ (50 mL). The organic layer was separated, and the aqueous layer was extracted with CH_2Cl_2 (50 mL × 4). The organic layers were combined, dried over anhydrous $MgSO_4$, and concentrated *in vacuo*. The residue was purified by PTLC twice (silica gel, CH_2Cl_2/MeOH = 15:1 for each) to afford 76.3 mg of the title product **14** in 44% yield. ^{1}H NMR (270 MHz, $CDCl_3$) δ 7.20–6.76 (4H, m), 6.65 (1H, d, J = 8.24 Hz), 4.84 (1H, d, J = 13.0 Hz), 4.22–3.78 (4H, m), 3.30–3.15 (1H, m), 2.97–2.90 (2H, m), 2.78–2.58 (2H, m), 2.35–2.33 (3H, m), 1.90–1.50 (4H, m). MS (ESI positive) m/z: $[M+H]^+$ 403.

4.1.3.5. 5-Chloro-3-{[4-(4-fluoro-2-methylphenyl)piperidin-1-yl]methyl}-1,2,3,4-tetrahydroisoquinolin-8-ol (15), general procedure of borane reduction of amide for amine synsthesis. To a solution of compound **14** (76.3 mg, 0.189 mmol) in anhydrous THF (3.7 mL) was

added a solution of $BH_3 \cdot SMe_2$ (1.0 M in THF, 90 μL, 90 μmol) at room temperature under N_2. The reaction solution was warmed up to reflux conditions, stirred under N_2 for 5 h, cooled to room temperature, then more $BH_3 \cdot SMe_2$ (1.0 M in THF, 90 μL, 90 μmol) was added. Again, the reaction solution was warmed up to reflux conditions, stirred for 24 h, then cooled to room temperature, then more $BH_3 \cdot SMe_2$ (1.0 M in THF, 90 μL, 90 μmol) was added. The reaction solution warmed up to reflux conditions, stirred for 16 h, cooled to 0 °C, then 6 N HCl (1.26 mL), 2 N HCl (1.0 mL), and MeOH (3.7 mL) were added dropwise. The resulting mixture was warmed up to reflux conditions, stirred under N_2 for 24 h, then allowed to room temperature. The resulting solution was diluted with MeOH (10 mL), then concentrated *in vacuo*. For the residue, a procedure, that consists of the addition of MeOH (5 mL) followed by the concentration of the resulting mixture *in vacuo*, was repeated six times. The residue was dissolved in CH_2Cl_2 (25 mL)–MeOH (3 mL), then poured into saturated aqueous $NaHCO_3$ (15 mL)–H_2O (10 mL). The organic layer was separated, and the aqueous layer was extracted with CH_2Cl_2–MeOH (10:1, 25 mL × 2), and with CH_2Cl_2 (25 mL × 2). The organic layers were combined, dried over anhydrous $MgSO_4$, and concentrated *in vacuo*. The residue was purified by column chromatography (silica gel, CH_2Cl_2/MeOH = 15:1, then CH_2Cl_2/MeOH/25% aqueous ammonia = 15:1:0.15) followed by PTLC (silica gel, CH_2Cl_2/MeOH/25% aqueous ammonia = 18:1:0.1 × 2, that is, twice developments on the same plate) was performed to afford 26.3 mg of the title product **15** in 36% yield as a slight yellowish-white solid. ^{1}H NMR (300 MHz, $CDCl_3$) δ 7.19–7.14 (1H, m), 6.99 (1H, d, J = 8.40 Hz), 6.90–6.84 (2H, m), 6.47 (1H, d, J = 8.43 Hz), 4.30 (2H, br s), 4.14 (1H, d, J = 15.9 Hz), 3.76 (1H, d, J = 15.9 Hz), 3.13–1.73 (17H, m, including 3H, s, at 2.32 ppm). MS (ESI positive) m/z: $[M+H]^+$ 389 for salt-free form. Monocitrate of compound **15:** Anal. ($C_{22}H_{26}ClFN_2O \cdot C_6H_8O_7$) C, H, N.

4.1.4. Synthesis of 1′-(1,2,3,4-tetrahydroisoquinolin-3-ylcarbonyl)-2,3-dihydro-1′*H*-spiro[indene-1,4′-piperidine] (18) and 1′-[(1,2,3,4-tetrahydroisoquinolin-3-yl)methyl]-2,3-dihydro-1′*H*-spiro[indene-1,4′-piperidine] (19).

4.1.4.1. *tert*-Butyl 3-(2,3-dihydro-1′*H*-spiro[indene-1,4′-piperidin]-1′-ylcarbonyl)-3,4-dihydroisoquinoline-2(1*H*)-carboxylate (17). To a stirred solution of compound **2** (610.1 mg, 2.20 mmo), 2,3-dihydrospiro[indene-1,4′-piperidine] hydrochloride (492.2 mg, 2.20 mmol), dry Et_3N (307 μL, 2.20 mmol), and HOBT (327.0 mg, 2.42 mmol) in dry DMF (15.0 mL) and anhydrous THF (10.0 mL) was added WSCI (463.9 mg, 2.42 mmol) at a time at –20 °C under N_2. The resulting mixture was allowed to warm to room temperature, and stirred under N_2 for 2 days, and the mixture was turned into yellow solution during the reaction. After some of the solvent were reduced on a rotary evaporator, the residue was poured into aqueous $NaHCO_3$ (200 mL) at 0 °C, and the resulting mixture was extracted with Et_2O (100 mL × 2). The combined extracts were washed with H_2O (70 mL), dried over anhydrous $MgSO_4$, filtered, and concentrated *in vacuo*. The residue was purified by column chromatography (silica gel, hexane/AcOEt = 2:1) to afford 785.8 mg of the title product **17** in 80% yield as a white foamy solid. ^{1}H NMR (300 MHz, $CDCl_3$) δ 7.25–7.04 (8H, m), 5.47–5.27 and 5.08–4.73 (total 2H, each m), 4.65–4.35 and 4.10–3.90 (total 3H, each m), 3.40–2.70 (6H, m), 2.18–2.02 (2H, m), 2.00–1.40 (13H, m, including 9H, s at 1.49 ppm).

4.1.4.2. 1′-(1,2,3,4-Tetrahydroisoquinolin-3-ylcarbonyl)-2,3-dihydro-1′*H*-spiro[indene-1,4′-piperidine] (18). A mixture of compound **17** (154.2 mg, 0.345 mmol) and 10% HCl solution in MeOH (15.0 mL) was stirred at room temperature under N_2 for 16 h. After evaporation of the solvent, the residue was partitioned between CH_2Cl_2 (30 mL) and saturated aqueous $NaHCO_3$ (30 mL) at 0 °C. The organic layer was separated, and the aqueous layer was extracted with CH_2Cl_2 (30 mL × 3). The organic layers were combined, washed with brine, dried over anhydrous $MgSO_4$, filtered, and concentrated *in vacuo* to afford 120.8 mg of the title product **18** in quantitative yield. ^{1}H NMR (270 MHz, $CDCl_3$) δ 7.26–7.02 (8H, m), 4.74–4.59 (1H, m), 4.14 (2H, br s), 4.04–3.91 (2H, m), 3.40–3.24 (1H, m), 3.12–2.79 (5H, m, including 2H, t, J = 7.26 Hz at 2.95 ppm), 2.33 (1H, br s), 2.12 (2H, t, J = 7.24 Hz), 2.00–1.73 (2H, m), 1.70–1.55 (2H, m). **Hydrochroride salt formation, general procedure** [3,4]: A solution

of compound **18** (8.9 mg) in CH_2Cl_2 (10 mL) and excess equivalent of 10% HCl/MeOH solution (20 mL) was stirred at room temperature for 30 min, and then concentrated *in vacuo*. The resulting solid was collected and dried under vacuum at 50 °C for 6 h to give hydrochloride salt as a white solid. Hydrochloride salt of compound **18:** MS (ESI positive) m/z: $[M+H]^+$ 347.16.

4.1.4.3. 1′-[(1,2,3,4-Tetrahydroisoquinolin-3-yl)methyl]-2,3-dihydro-1′*H*-spiro[indene-1,4′-piperidine] (19), typical procedure. To a stirred solution of the above compound **18** (salt free, 111.9 mg, 0.323 mmol) in anhydrous THF (3.0 mL) was added LAH (36.8 mg, 0.970 mmol) at 0 °C under N_2. The reaction mixture was stirred at 0 °C under N_2 for 30 min, allowed to warm to room temperature, and stirred for 16 h. The reaction mixture was cooled to 0 °C, then AcOEt (20 mL) was added at the temperature under N_2. The resulting mixture was stirred for 15 min at 0 °C, ice-cooled H_2O (15 mL) was added dropwise at the temperature, and then the resulting mixture was stirred at 0 °C for 30 min. The organic layer was separated, and the aqueous layer was extracted with AcOEt (20 mL × 3). The organic layers were combined, dried over anhydrous $MgSO_4$, filtered, and concentrated *in vacuo*. The residue was purified by PTLC (silica gel, CH_2Cl_2/MeOH/25% NH_4OH = 150:10:1) to afford 85.0 mg of the title product **19** in 79% yield as a slight brownish-white solid. ^{1}H NMR (300 MHz, $CDCl_3$) δ 7.24–7.02 (8H, m), 4.10 (2H, s), 3.13–3.03 (1H, m), 2.99–2.79 (4H, m, including 2H, t, J = 7.50 Hz at 2.90 ppm), 2.72 (1H, dd, J = 15.9 Hz, J = 3.84 Hz), 2.60–2.25 (5H, m), 2.18–2.09 (1H, m), 2.04–1.88 (4H, m, including 2H, t, J = 7.50 Hz at 2.02 ppm), 1.58–1.50 (2H, m). Monocitrate of compound **19:** IR (KBr): 3400, 1717, 1589, 1456, 1440, 1393, 1209, 758 cm^{-1}. MS (ESI positive) m/z: $[M+H]^+$ 333.18. Anal. ($C_{23}H_{28}N_2 \cdot C_6H_8O_7$) C, H, N.

4.1.5. Synthesis of 1′-[(2-methyl-1,2,3,4-tetrahydroisoquinolin-3-yl)methyl]-2,3-dihydro-1′*H*-spiro[indene-1,4′-piperidine] (20) and 3-{(2,3-dihydro-1′*H*-spiro[indene-1,4′-piperidin]-1′-yl)methyl}-2-methyl-3,4-dihydroisoquinolin-1(2*H*)-one (21).

4.1.5.1. 1′-[(2-Methyl-1,2,3,4-tetrahydroisoquinolin-3-yl)methyl]-2,3-dihydro-1′*H*-spiro[indene-1,4′-piperidine] (20). To a stirred solution of compound **17** (179.0 mg, 0.401 mmol) in anhydrous THF (5.0 mL) was added LAH (68.3 mg, 1.80 mmol) at room temperature under N_2 [4]. The reaction mixture was stirred at room temperature for 16 h, cooled to 0 °C, AcOEt (10 mL) was added at the temperature under N_2, allowed to warm to room temperature, and stirred for 30 min at room temperature. The reaction mixture was cooled to 0 °C, ice-cooled H_2O (15 mL) was added at the temperature, and the resulting mixture was stirred at 0 °C for 30 min. The organic layer was separated, and the aqueous layer was extracted with AcOEt (15 mL × 3). The organic layers were combined, dried over anhydrous $MgSO_4$, filtered, and concentrated *in vacuo*. The residue was purified by PTLC (silica gel, CH_2Cl_2/MeOH = 10:1) to afford 61.2 mg of the title product **20** in 44% yield. ^{1}H NMR (270 MHz, $CDCl_3$) δ 7.25–7.09 (7H, m), 7.06–7.00 (1H, m), 3.84 (1H, d, J = 15.8 Hz), 3.74 (1H, d, J = 16.0 Hz), 3.03–2.71 (7H, m, including 2H, t, J = 7.24 Hz at 2.89 ppm), 2.64 (1H, dd, J = 12.4 Hz, J = 4.94 Hz), 2.48 (3H, s), 2.37–2.10 (3H, m), 2.05–1.87 (4H, m, including 2H, t, J = 7.24 Hz at 2.01 ppm), 1.57–1.47 (2H, m). Hydrochloride salt of compound **20:** MS (ESI positive) m/z: $[M+H]^+$ 347.

4.1.5.2. 3-{(2,3-Dihydro-1′*H*-spiro[indene-1,4′-piperidin]-1′-yl)methyl}-2-methyl-3,4-dihydroisoquinolin-1(2*H*)-one (21). To a stirred mixture of compound **20** (salt free, 49.0 mg, 0.141 mmol) and anhydrous $MgSO_4$ (29.5 mg, 0.245 mmol) in acetone (3.6 mL)–H_2O (1.8 mL) was added $KMnO_4$ (38.8 mg, 0.245 mmol) at room temperature under N_2 [23]. The reaction mixture was stirred at room temperature under N_2 for 1 h, then filtered. After the filtrate was concentrated on a rotary evaporator, the resulting aqueous residue was extracted with CH_2Cl_2 (25 mL × 3). The combined extracts were dried over anhydrous $MgSO_4$, and concentrated *in vacuo*. The residue was purified by PTLC (silica gel, CH_2Cl_2/MeOH = 10:1) to afford 11.8 mg of the title product **21** in 23% yield. ^{1}H NMR (300 MHz, $CDCl_3$) δ 8.08–7.18 (8H, m), 3.66 (1H, m), 3.35–3.26 (1H, m), 3.22 (3H, s), 3.11–2.62 (5H, m), 2.45–1.47 (10H, m). MS (EI direct) m/z: M^+ 360 for salt-free form. Hydrochroride salt of compound **21:** MS (ESI positive) m/z: $[M+H]^+$ 361.19.

4.1.6. Synthesis of 1′-[(2-acetyl-1,2,3,4-tetrahydroisoquinolin-3-yl)methyl]-2,3-dihydro-1′*H*-spiro[indene-1,4′-piperidine] (22). To a stirred solution of compound **19** (salt free, 71.7 mg, 0.216 mmol) and dry Et_3N (75.3 μL, 0.547 mmol) in dry CH_2Cl_2 (2.0 mL) was added acetyl chloride (15.4 μL, 0.217 mmol) at room temperature under N_2. The resulting reaction mixture was warmed up to reflux conditions, stirred under N_2 for 3 h, cooled to 0 °C, then ice-cooled H_2O (20 mL) was added. The resulting mixture was extracted with CH_2Cl_2 (25 mL × 3), and the combined extracts were washed with brine, dried over anhydrous $MgSO_4$, filtered, and concentrated *in vacuo*. The residue was purified by PTLC (silica gel, CH_2Cl_2/MeOH = 20:1) to afford 74.8 mg of the title product **22** in 92% yield. ^{1}H NMR (300 MHz, $CDCl_3$) δ 7.25–7.08 (8H, m), 5.25–5.15 (0.4H, m), 5.14 (0.6H, d, J = 17.8 Hz), 4.64 (0.4H, d, J = 16.3 Hz), 4.49 (0.4H, d, J = 16.1 Hz), 4.34–4.20 (0.6H, m), 4.25 (0.6H, d, J = 18.3 Hz), 3.13–2.64 (6H, m), 2.43–2.34 (1H, m), 2.32–2.09 (6H, m), 2.02–1.78 (4H, m), 1.53–1.43 (2H, m). Hydrochroride salt of compound **22:** MS (ESI positive) m/z: $[M+H]^+$ 375.22. Anal. ($C_{25}H_{30}N_2O\cdot HCl$) C, H, N.

4.1.7. Synthesis of 5-chloro-3-{(2,3-dihydro-1′*H*-spiro[indene-1,4′-piperidin]-1′-yl)methyl}-1,2,3,4-tetrahydroisoquinolin-8-ol (23). Compound **11** (crude, see section 4.1.3.2.) was coupled with 2,3-dihydrospiro[indene-1,4′-piperidine] hydrochloride according to the procedure for the synthesis of compound **3** from compounds **1** and **2** in section 4.1.2.1., then deprotected of the *N*-Boc portion of the resulting amide according to the procedure for the synthesis of compound **4** from compound **3** in section 4.1.2.2., followed by $BH_3\cdot$SMe reduction of the amido portion to afford the title product **23** according to the procedure for the synthesis of compound **15** from compound **14** in section 4.1.3.5. Overall yield was 51%.

Compound **23:** ^{1}H NMR (300 MHz, DMSO-d_6) δ 9.60 (1H, br s), 7.27–7.10 (4H, m), 7.06 (1H, d, J = 8.4 Hz), 6.64 (1H, d, J = 9.0 Hz), 3.96 (1H, d, J = 15.6 Hz), 3.63 (1H, d, J = 16.8 Hz), 3.00–2.65 (7H, m, including 2H, t, J = 7.3 Hz at 2.85 ppm), 2.45–2.37 (2H, m), 2.30–2.05 (3H, m), 1.97 (2H, t, J = 7.2 Hz), 1.93–1.80 (2H, m), 1.50–1.40 (2H, m). Monocitrate of compound **23:** MS (ESI positive) m/z: $[M+H]^+$

383. IR (KBr): 2945, 1719, 1600, 1456, 1340, 1298, 1192, 760 cm^{-1}. Anal. ($C_{23}H_{27}ClN_2O \cdot C_6H_8O_7$) C, H, N.

4.1.8. Synthesis of 5-bromo-3-{(2,3-dihydro-1′*H*-spiro[indene-1,4′-piperidin]-1′-yl)methyl}-1,2,3,4-tetrahydroisoquinolin-8-ol (25). To a suspension of *m*-tyrosine (1.00 g, 5.50 mmol) in AcOH (100 mL) was added dropwise bromine (312 μL, 6.05 mmol) in AcOH (100 mL) at room temperature under N_2. The reaction mixture was stirred at room temperature under N_2 for 2 h. The resulting solid was collected by filtration, washed with hexane, and dried under vacuum to afford 2.24 g of 2-bromo-5-hydroxyphenylalanine as a white solid (crude). A mixture of 2-bromo-5-hydroxyphenylalanine (2.0 g, crude) and 37% formalin (10 mL) in H_2O (10.0 mL) was stirred at 90 °C under N_2 for 2 h. After cooling to room temperature, the resulting solid was collected by filtration, washed with H_2O, and dried under vacuum to afford 668.0 mg of 5-bromo-8-hydroxy-1,2,3,4-tetrahydroisoquinoline-3-carboxylic acid **24** [22] as a white solid (crude) (see also section 4.1.3.2. for the synthesis of compound **11**).

After compound **24** was *N*-Boc protected according to the procedure for the synthesis of compound **11** from compound **10** in section 4.1.3.2., the resulting *N*-Boc protected carboxylic acid was coupled with compound **16** according to the procedure for the synthesis of compound **3** from compounds **1** and **2** in section 4.1.2.1., then the *N*-Boc portion of the resulting amide was deprotected according to the procedure for the synthesis of compound **4** from compound **3** in section 4.1.2.2., followed by reduction of the amido portion with $BH_3 \cdot SMe$ to afford the title product **25** according to the procedure for the synthesis of compound **15** from compound **14** in section 4.1.3.5. Overall yield was 11%. Compound **25:** ^{1}H NMR (270 MHz, DMSO-d_6) δ9.60 (1H, br s), 7.28–7.09 (5H, m), 6.60 (1H, d, J = 8.6 Hz), 3.96 (1H, d, J = 16.3 Hz), 3.63 (1H, d, J = 16.5 Hz), 2.98–2.75 (4H, m), 2.70–1.78 (12H, m), 1.50–1.40 (2H, m). Monocitrate of compound **25:** MS (ESI positive) m/z: 429, 427 $(M+H)^+$. IR (KBr): 1719, 1585, 1477, 1448, 1296, 1186 cm^{-1}. Anal. ($C_{23}H_{27}BrN_2O \cdot C_6H_8O_7$) C, H, N.

4.1.9. Synthesis of 3-{(2,3-dihydro-1′*H*-spiro[indene-1,4′-piperidin]-1′-yl)methyl}-1,2,3,4-tetrahydroisoquinolin-8-ol (27). A mixture of compound **25** (salt free, 140.0 mg, 0.328 mmol), Boc_2O (179 mg, 0.820 mmol) and 2 N NaOH (5.0 mL, 10 mmol) in 1,4-dioxane (5.0 mL) was stirred at room temperature under N_2 for 4 days. The reaction mixture was washed with H_2O (20 mL) and brine (20 mL), dried over anhydrous Na_2SO_4, filtered and concentrated *in vacuo* to give 145.6 mg of *N*-Boc compound as a pale yellow amorphous solid (crude). A mixture of the above *N*-Boc compound (145.0 mg, crude) and 5% Pd/C (15 mg) in dry MeOH (20 mL) was stirred at room temperature under H_2 at 1.0–4.0 atm for 16 h [35]. After removal of the catalyst by filtrated through Celite pad, the filtrate was concentrated *in vacuo*. The residue was purified by column chromatography (silica gel, CH_2Cl_2/MeOH/25% aqueous ammonia = 400:10:1) to afford 64.3 mg of *tert*-butyl 3-{(2,3-dihydro-1′*H*-spiro[indene-1,4′-piperidine]-1′-yl)methyl}-8-hydroxy-3,4-dihydroisoquinolin-2(1*H*)-carboxylate **26** in 44% from compound **25**.

A mixture of compound **26** (64.0 mg, 0.143 mmol) and 10% HCl solution in MeOH (3.0 mL) was stirred at room temperature under N_2 for 18 h, then concentrated *in vacuo*. The residue was basified by addig 2 N NaOH, then the resulting mixture was extracted with AcOEt (100 mL). The extract was washed with brine, dried over anhydrous Na_2SO_4, filtered, and concentrated *in vacuo* to afford 49.8 mg of the title product **27** in 100% yield as a brown amorphous solid. ^{1}H NMR (270 MHz, $CDCl_3$) δ 7.28–7.11 (4H, m), 6.92 (1H, dd, *J* = 7.8 Hz, *J* = 7.7 Hz), 6.61 (1H, d, *J* = 7.4 Hz), 6.55 (1H, d, *J* = 7.9 Hz), 4.23 (1H, d, *J* = 15.8 Hz), 3.89 (1H, d, *J* = 16.0 Hz), 3.20–3.05 (1H, m), 3.00–2.30 (10H, including 2H, t, *J* = 7.2 Hz at 2.89 ppm), 2.20–1.90 (5H, m, including 2H, t, *J* = 7.3 Hz at 2.00 ppm), 1.60–1.47 (2H, m). Monocitrate of compound **27:** MS (ESI positive) m/z: 349 $(M+H)^+$. IR (KBr): 3200, 1719, 1597, 1472, 1439, 1375, 1342, 1283 cm^{-1}. Anal. ($C_{23}H_{30}N_2O \cdot C_6H_8O_7$) C, H, N.

4.1.10. Synthesis of 3-{(2,3-dihydro-1′*H*-spiro[indene-1,4′-piperidin]-1′-yl)methyl}-1,2,3,4-tetrahydroisoquinolin-6-ol (30).

4.1.10.1. *tert*-Butyl 3-(2,3-dihydro-1′*H*-spiro[indene-1,4′-piperidin]-1′-ylcarbonyl)-6-hydroxy-3,4-dihydroisoquinoline-2(1*H*)-carboxylate (29). A mixture of 6-hydroxy-1,2,3,4-

tetrahydroisoquinoline-3-carboxylic acid **28** (500 mg, 2.59 mmol) that was prepared by reported method [24], Boc_2O (622 mg, 2.85 mmol), and anhydrous Na_2CO_3 (1.4 g, 13 mmol) in 1,4-dioxane (10 mL) and H_2O (20 mL) was stirred at room temperature under N_2 for 3 days. The reaction mixture was acidified with 2 N HCl (pH 3) and extracted with AcOEt (150 mL). The combined extracts were washed with H_2O (50 mL) and brine (50 mL), dried over anhydrous Na_2CO_3, filtered, and concentrated *in vacuo* to give 760 mg of *N*-Boc derivative as a colorless amorphous solid, containing a by-product that would be *N*,*O*-di-Boc derivative of compound **28** (not isolated).

A mixture of the above Boc derivatives (144 mg, crude), 2,3-dihydrospiro[indene-1,4′-piperidine] hydrochloride (100 mg, 0.447 mmol), WSCI (94 mg, 0.492 mmol), dry Et_3N (0.07 mL, 0.492 mmol), and HOBT (66 mg, 0.492 mmol) in dry DMF (5 mL) was stirred at room temperature for 4 days. The reaction mixture was diluted with AcOEt (100 mL), washed with H_2O (30 mL), dried over anhydrous Na_2SO_4, filtered, and concentrated *in vacuo* to give 340 mg of yellow gum. The residue was purified by column chromatography (silica gel, hexane/AcOEt = 2:1) to afford 159.2 mg of the title product **29** as a white amorphous solid in 77% yield from 2,3-dihydrospiro[indene-1,4′-piperidine] hydrochloride. ^{1}H NMR (270 MHz, $CDCl_3$) δ9.23 (1H, br s), 7.80–7.67 (1.5H, m), 7.47–7.36 (1.5H, m), 7.25–7.10 (2.5H, m), 6.86 (0.5H, d, J = 7.9 Hz), 6.70–6.53 (1H, m), 5.40–5.20, 5.05–4.25, and 4.18–3.93 (total 5H, each m), 3.45–2.70 (6H, m), 2.15–1.40 (15H, m, including 9H, s at 1.47 ppm); MS (EI direct) m/z: M^+ 462.

4.1.10.2. 3-{(2,3-Dihydro-1′*H*-spiro[indene-1,4′-piperidin]-1′-yl)methyl}-1,2,3,4-tetrahydroisoquinolin-6-ol (30). After deprotection of *N*-Boc group of compound **29** was performed to afford (2,3-dihydro-1′*H*-spiro[indene-1,4′-piperidine]-1′-yl)(6-hydroxy-1,2,3,4-tetrahydroisoquinolin-3-yl)methanone according to the procedure for the synthesis of compound **4** from compound **3** in section 4.1.2.2., the amido portion of the resulting compound was reduced with BH_3·SMe to afford the title product **30** according to the procedure for the synthesis of compound **15** from compound **14** in section 4.1.3.5. Overall yield was 63%. Compound **30:** ^{1}H NMR (270 MHz, DMSO-d_6) δ9.05 (1H, br s), 7.30–

7.10 (4H, m), 6.83 (1H, d, *J* = 8.3 Hz), 6.55–6.46 (2H, m), 3.84 (2H, s), 3.04–2.74 (4H, m), 2.65–1.78 (12H, m), 1.50–1.40 (2H, m).

This solid (53.5 mg) was converted to citric acid salt similar to that described above to afford 74.6 mg of citric acid salt as a white amorphous solid. Monocitrate of compound **30:** MS (EI direct) m/z: M^+ 348. IR (KBr): 1720, 1578, 1508, 1477, 1456, 1389, 1306, 1242 cm^{-1}. Anal. ($C_{23}H_{28}N_2O \cdot C_6H_8O_7$) C, H, N.

4.1.11. Synthesis of 1′-{(3,4-dihydro-2*H*-chromen-3-yl)methyl}-2,3-dihydro-1′*H*-spiro[indene-1,4′-piperidine] (33).

4.1.11.1. 1′-(3,4-Dihydro-2*H*-chromen-3-ylcarbonyl)-2,3-dihydro-1′*H*-spiro[indene-1,4′-piperidine] (32). To a mixture of 2,3-dihydrospiro[indene-1,4′-piperidine] hydrochloride (89.5 mg 0.400 mmol), chromane-3-carboxylic acid (92.7 mg, 0.520 mmol), WSCI (127.3 mg, 0.664 mmol), and HOBT (101.7 mg, 0.664 mmol) was added dry Et_3N (174 μL, 1.25 mmol) in dry DMF (3.0 mL) at room temperature under N_2. The reaction mixture was stirred at room temperature under N_2 for 24 h. The reaction mixture was partitioned between diethyl ether (15 mL) and H_2O (15 mL). The ethereal layer was separated, and the aqueous solution was extracted with diethyl ether (15 mL × 2). The ethereal layers were combined, dried over anhydrous $MgSO_4$, and concentrated *in vacuo*. The residue was purified by PTLC (silica gel, hexane/AcOEt = 3:1) was performed to afford 101.7 mg of the title product **32** in 73% yield. ^{1}H NMR (300 MHz, $CDCl_3$) δ 7.25–7.07 (6H, m), 6.90–6.83 (2H, m), 4.70–4.37 (2H, m), 4.16–3.96 (2H, m), 3.39–3.12 (3H, m), 2.96 (2H, t, *J* = 7.50 Hz), 2.90–2.79 (2H, m), 2.12 (2H, t, *J* = 7.50 Hz), 1.83–1.58 (4H, m).

4.1.11.2. 1′-[(3,4-Dihydro-2*H*-chromen-3-yl)methyl]-2,3-dihydro-1′*H*-spiro[indene-1,4′-piperidine] (33). To a solution of compound **32** (101.7 mg, 0.293 mmol) in anhydrous THF (5.0 mL) was added LAH (24.4 mg, 0.643 mmol) at 0 °C under N_2. The reaction mixture was stirred at the same temperature for 30 min, allowed to warm to room temperature, and stirred for 1 day. The reaction mixture was cooled to 0 °C, AcOEt (15 mL) was added dropwise under N_2, stirred at 0 °C for 10 min,

allowed to warm to room temperature, and stirred for 1 h. The mixture was cooled to 0 °C, ice-cooled H_2O (25 mL) was added dropwise, and the resulting mixture was stirred at 0 °C for 1 h. The organic layer was separated, and the aqueous layer was extracted with AcOEt (25 mL × 4). The organic layers were combined, dried over anhydrous $MgSO_4$, and concentrated *in vacuo*. The residue was purified by PTLC (silica gel, hexane/AcOEt = 5:1) to afford 90.4 mg of the title product **33** in 93% yield. ^{1}H NMR (300 MHz, $CDCl_3$) δ 7.24–7.05 (6H, m), 6.87–6.80 (2H, m), 4.36–4.31 (1H, m), 3.90–3.83 (1H, m), 2.91–2.80 (5H, m), 2.58–1.50 (12H, m). **4-Toluenesulfonic acid salt formation:** Compound **33** (90.4 mg, 0.271 mmol) and one equivalent of 4-toluenesulfonic acid monohydrate (51.6 mg, 0.271 mmol) was dissolved in dry MeOH (30 mL) and dry CH_2Cl_2 (30 mL), and the resulting solution was stirred at room temperature under N_2 for 2 h, then concentrated *in vacuo*. The residue was suspended in dry CH_2Cl_2–dry hexane–anhydrous Et_2O, and concentrated *in vacuo*. The resulting solid was collected by filtration, and dried under vacuum at 60 °C for 2 h to afford 110 mg of 4-toluenesulfonate salt as a white solid. Mono-4-toluenesulfonate of compound **33:** Anal. ($C_{23}H_{27}NO \cdot C_7H_8O_3S$) C, H, N.

4.1.12. High-speed parallel synthesis of 1′-(substituted methyl)-spiro[indane-1,4′-piperidine] derivatives using amidation followed by reduction for multi-analog productions.

(1) Reaction. To carboxylic acid (75 μmol) in 1,2-dichloroethane (0.5 mL) was added 1,2-dichloroethane (0.5 mL) solution of 2,3-dihydrospiro[indene-1,4′-piperidine] hydrochloride (50 μmol) and dry Et_3N (50 μmol), then added *N*-cyclohexylcarbodiimide-*N*′-methyl PS resin (42 mg, 100 μmol). The reaction mixture was then stirred at room temperature for 23 h. The reaction mixture was filtered and washed with MeOH (1 mL), then the eluate was analyzed by LS/MS and concentrated to dryness by N_2 gas blow and vacuum centrifuge to give crude amide intermediate. To crude amide (50 μmol) in anhydrous THF (0.5 mL) was added 1 M solution of LAH in Et_2O (250 μmol/250 μL). The reaction mixture was then stirred at room temperature for 10 min. The mixture was quenched by H_2O (20 μL) and 10% MeOH–CH_2Cl_2 (1 mL), then filtered through anhydrous Na_2SO_4 (1 g) and SiO_2 (100 mg)

column preconditioned with 10% MeOH–CH_2Cl_2 (0.5 mL) solution, and then washed with 10% MeOH–CH_2Cl_2 (1.5 mL). Dispersion of reagents (to set reaction) and filtration (after reaction) were performed by hand and by a Gilson 215 liquid handler, respectively. The eluate was analyzed by LS/MS and concentrated to dryness by N_2 gas blow to afford the desired product. In case it was needed, the products were purified with preparative LC/MS to give the desired products as formate form or salt-free form dependent on the purification condition. (2) HPLC/LC–MS method. (i) Analytical condition: equipment: Waters 2690; column: Shiseido C18 UG80 or C18 MG120, 5 μm, 4.6 × 50 mm; column temp: 40 °C; detector: photodiodearray (210–400 nm); flow: 1.0 mL/min; solvent (a) as acidic condition, A: 0.1% HCO_2H; B: MeOH, gradient; solvent (b) as basic condition, A: 10 mM aqueous NH_4OAc; B: MeOH, gradient; MS condition: ionization method: ESI (positive). (ii) Preparative conditions: equipment: Shimadzu LC10 system or Waters prep LC/MS system; column: Shiseido C18 SG120, 5 μm, 20 × 50 mm; column temp: 40 °C; flow: 1.0 mL/min; solvent (a) as acidic condition, A: 0.1% HCO_2H; B: MeOH, gradient; solvent (b) as basic condition, A: 10 mM aqueous NH_4OAc; B: MeOH, gradient; peak detection: UV 250 nm.

In the parallel synthesis utilizing the above protocol (1) and (2), a formate salt of 1′-[(1,2,3,4-tetrahydronaphthalen-2-yl)methyl]-2,3-dihydro-1′*H*-spiro[indene-1,4′-piperidine] **38** was prepared from 2,3-dihydrospiro[indene-1,4′-piperidine] hydrochloride and 1,2,3,4-tetrahydronaphthalene-2-carboxylic acid.

4.2. Biology

4.2.1. Characterization of NOP receptor antagonists *in vitro*.

In vitro studies of synthetic compounds for hNOP receptor binding affinities and human μ receptors binding affinities, and for antagonist activities against N/OFQ stimulated [^{35}S]GTPγS binding were conducted [6,7,25].

4.2.1.1. Materials. The hNOP receptor transfected human embryonic kidney (HEK)-293 cell membranes and the human μ receptor transfected Chinese hamster ovary (CHO)-K1 cell membranes were purchased from Receptor Biology Inc., respectively. [^{3}H]N/OFQ (150 Ci/mmol), [^{35}S]GTPγS (1060–1150 Ci/mmol) and wheatgerm agglutinin (WGA)-scintillation proximity assay (SPA) beads were obtained from Amersham Pharmacia Biotech K.K., and [^{3}H]DAMGO (54.0 Ci/mmol) was provided from NEN^{TM} Life Science Products Inc., respectively. N/OFQ was from Peptide Institute Inc. DAMGO was from Sigma-Aldrich, respectively.

4.2.1.2. Evaluation of receptor binding affinities to hNOP receptor and human μ receptor. All competitive displacement analyses (IC_{50} and K_i) for the hNOP receptor and human μ receptor were performed in duplicate in a 96-well plate using a scintillation proximity assay (SPA), respectively. After the reaction, the assay plate was centrifuged at 1,000 rpm for 1 min, and then the radioactivity was measured by a 1450 MicroBeta^{TM} (Wallac) liquid scintillation counter. IC_{50} values were calculated by nonlinear regression with the software GraphPad Prism version 4.0 (GraphPad Software, Inc., San Diego, USA), respectively. K_i values were calculated by the following equation, $K_i = IC_{50}/(1 + [L]/K_D)$, where [L] is the radiolabeled ligand concentration and K_D is the dissociation constant.

4.2.1.2.1. hNOP receptor binding assay. The hNOP receptor membranes (8.3 μg) were incubated at 25 °C for 45 min with 0.4 nM [^{3}H]N/OFQ, 1.0 mg of WGA-SPA beads, and six different concentrations of compounds (10^{-11}–10^{-5} M, 10-fold) in a final volume of 0.2 mL of 50 mM HEPES buffer, pH 7.4, containing 10 mM $MgCl_2$ and 1 mM EDTA. Nonspecific binding was determined by the addition of 1 μM unlabeled N/OFQ. Approximately 900 cpm of total binding were obtained, of which 3.3% was the non-specific binding.

4.2.1.2.2. Human μ receptor binding assay. The human μ receptor membranes (18 μg) were incubated at 25 °C for 45 min with 1.0 nM [^{3}H]DAMGO, 1.0 mg of WGA-SPA beads, and six different concentrations of compounds (10-fold) in a final volume of 0.2 mL of 50 mM Tris–HCl buffer, pH 7.4, containing 5 mM $MgCl_2$. Nonspecific binding was determined by the addition of 1 μM of unlabeled DAMGO. Approximately 240 cpm of total binding were obtained, of which 9.6% was the non-specific binding.

4.2.1.3. Evaluation of antagonist activities against N/OFQ-stimulated [^{35}S]GTPγS binding. [^{35}S]GTPγS binding to the hNOP receptor expressed HEK-293 cell membranes was performed according to the method of SPA G-protein-coupled receptor assay provided by Amersham Biosciences with slight modification. For evaluation of antagonism activities (IC_{50}), the membranes were incubated at 25 °C for 1.5 h with 10 nM N/OFQ and various concentrations of compounds in assay buffer (400 pM [^{35}S]GTPγS, 5 μM GDP, 20 mM HEPES, 100 mM NaCl, 5 mM $MgCl_2$, 1 mM EDTA, pH 7.4) containing 1.5 mg of WGA-SPA beads in a final volume of 200 μL. All assays were performed in duplicate. Each compound was tested at six different concentrations ranging from 0.1 nM to 10 μM. Membrane-bound radioactivity was detected by scintillation counting using Wallac 1450 MicroBeta^{TM}. Basal binding was determined in the absence of ligands and non-specific binding (NSB) was determined by the addition of unlabeled 10 μM GTPγS. Percent basal was defined as (stimulated binding – NSB)/(basal binding – NSB) ×100%. IC_{50} value of each compound against 10 nM N/OFQ stimulated-binding was calculated by nonlinear regression with GraphPad Prism version 4.0, respectively.

4.3. Pharmacokinetic study *in vitro*

4.3.1. General.

The apparatus of HPLC system was Agilent 1100 HPLC system, and MS/MS system was API-300 or API-3000. The analytical column was YMC polymer 18, 2.0 × 75 mm. The mobile phase consisted of 10 mM aqueous $AcONH_4$ and CH_3CN (20:80, v/v) or of 0.05% aqueous TFA and CH_3CN (20:80, v/v) was run at a flow rate of 0.35 mL/min. The column temperature was at 40 °C (ambient temperature with air conditioning, 24–25 °C). The sample in column eluent was detected by MS/MS.

4.3.2. Metabolic half-life values in human liver microsomes.

Test compounds (1.0 μM) were incubated in human liver microsomes (pooled human liver microsomes; protein concentration: 1.0 mg/mL) with 3.3 mM $MgCl_2$, 0.1 M $NaKHPO_4$ (pH 7.4), and NADPH-regenerating factors at 37 °C for various times on 96-deep well plates (final volume 600 μL). An aliquot of samples (50 μL) was collected at 0, 5, 15, 30, and 60 min after incubation and extracted with CH_3CN. The extracted samples were measured by HPLC/MS/MS system [3,5–7].

4.4. Evaluation of hERG potassium ion channel bindings *in vitro*

Cell paste of HEK-293 cells expressing the hERG product was suspended in 10-fold volume of ice-cold wash buffer (50 mM Tris base, 10 mM KCl, and 1 mM $MgCl_2$, adjusted pH 7.4). The cells were homogenized using a Polytron® homogenizer (Kinematica Inc.), and centrifuged at 48,000 × *g* for 20 min at 4 °C. The pellet was resuspended, homogenized and centrifuged once more in the same manner. The resultant supernatant was discarded, and the final pellet was resuspended (10-fold volume of ice-cold wash buffer) and then homogenized. The membrane homogenate was aliquoted and stored at –80 °C until use. The all manipulation was done on ice, and stock solution and equipment were kept on ice at all the time. For the saturation assay, experiments were conducted in a total volume of 200 μL in 96-well plates by Skatron method. It was determined by incubating 20 μL of [^{3}H]dofetilide and 160 μL of hERG homogenate (25–35 μg protein/well) at 22 °C for 60 min in incubation buffer. Total and non-

specific bindings (in the presence of 10 μM dofetilide) were determined in duplicate in a range of [^{3}H]dofetilide concentrations (1–50 nM). The incubations was terminated by rapid vacuum filtration over 0.2% polyethyleneimine soaked glass fiber filter paper using a Skatron cell harvester followed by three washes with ice-cold filtration buffer (50 mM Tris base, 10 mM KCl, and 1 mM $MgCl_2$, adjusted pH 7.4). Receptor-bound radioactivity was quantified by liquid scintillation counting using Packard LS counter. For the competition assay, 96-well plates were used, and a final assay volume was 200 μL. Various concentrations of test compounds (20 μL) were incubated in duplicate with 5 nM [^{3}H]dofetilide (36 μL), 1 mg/well SPA beads (34 μL) and 20 μg protein of hERG homogenate (110 μL) at 22 °C for 60 min in the incubation buffer. Nonspecific binding was determined by 10 μM dofetilide (20 μL). After the incubation, it was left for 3 h for settling beads. Channel-bound radioactivity was quantified by scintillation counting using Wallac MicroBeta plate counter. To define the radioligand concentration, 36 μL of the radioligand was mixed with Scintillation cocktail (Packard Aquasol-2, 3.5 mL) and the radioligand was counted on a Packard liquid scintillation analyzer (TRI-CARB 2700TR). All the binding data were analyzed by nonlinear regression with the software GraphPad Prism version 4.0 (GraphPad Software, Inc.) [3,5,7,25].

Appendix. Supplementary material

Supplementary data associated with this article can be found in the online version. These data include MOL files and InChiKeys of the most important compounds described in this article.

References and notes

1. (a) Meunier, J.-C.; Mollereau, C.; Toll, L.; Suaudeau, C.; Moisand, C.; Alvinerie, P.; Butour, J.-L.; Guillemot, J.-C.; Ferrara, P.; Monsarrat, B.; Mazarguil, H.; Vassart, G.; Parmentier, M.; Costentin, J. Isolation and structure of the endogenous agonist of opioid receptor-like ORL1 receptor, *Nature* **1995**, *377*, 532–535; (b) Reinscheid, R. K.; Nothacker, H.-P.; Bourson, A.; Ardati, A.; Henningsen, R. A.; Bunzow, J. R.; Grandy, D. K.; Langen, H.; Monsma, F. J. Jr.; Civelli, O. Orphanin FQ: a neuropeptide that activates an opioid-like G protein-coupled receptor, *Science* **1995**, *270*, 792–794; (c) Fukuda, K.; Kato, S.; Mori, K.; Nishi, M.; Takeshima, H.; Iwabe, N.; Miyata, T.; Houtani, T.; Sugimoto, T. cDNA cloning and regional distribution of a novel member of the opioid receptor family, *FEBS Lett.* **1994**, *343*, 42–46; (d) Mollereau, C.; Parmentier, M.; Mailleux, P.; Butour, J.-L.; Moisand, Christiane; Chalon, Pascale; Caput, D.; Vassart, G.; Meunier, J.-C. ORL1, a novel member of the opioid receptor family. Cloning, functional expression and localization, *FEBS Lett.* **1994**, *341*, 33–38; (e) Wang, J. B.; Johnson, P. S.; Imai, Y.; Persico, A. M.; Ozenberger, B. A.; Eppler, C. M.; Uhl, G. R., cDNA cloning of an orphan opiate receptor gene family member and its splice variant, *FEBS Lett.* **1994,** *348*, 75–79.

2. (a) Review: Calo', G.; Guerrini, R.; Rizzi A.; Salvadori, S.; Regoli, D. Pharmacology of nociceptin and its receptor: a novel therapeutic target, *Br. J. Pharmacol.* **2000**, *129*, 1261–1283; (b) Review: Mogil, J. S.; Pasternak, G. W. The molecular and behavioral pharmacology of the orphanin FQ/nociceptin peptide and receptor family, *Pharmacol. Rev.* **2001**, *53*, 381–415; (c) Review: Reinscheid, R. K.; Nothacker, H.-P.; Civelli, O. The orphanin FQ/nociceptine gene: structure, tissue distribution of expression and functional implications obtained from knockout mice, *Peptides* **2000,** *21*, 901–906; (d) Review: Mollereau, C.; Mouledous, L. Tissue distribution of the opioid receptor-like (ORL1) receptor, *Peptides* **2000**, *21*, 907–917; (e) Review: Meis, S. Nociceptin/orphanin FQ: Actions within the brain, *Neuroscientist* **2003**, *9*, 158–168; (f) Anthony, S. L.; Yung, H. W. Regulation of c-Jun N-terminal kinase by the ORL_1 receptor through multiple G proteins, *J. Pharmacol. Exp. Ther.* **2000,** *295*, 1094–1100; (g) Review: Donica, C. L.; Awwad, H. O.; Thakker, D. R.; Standifer, K. M. Cellular mechanisms

of nociceptin/orphanin FQ (N/OFQ) peptide (NOP) receptor regulation and heterologous regulation by N/OFQ, *Mol. Pharmacol.* **2013,** *83*, 907–918.

3. Hayashi, S.; Nakata, E.; Morita, A.; Mizuno, K.; Yamamura, K.; Kato, A.; Ohashi, K. Discovery of {1-[4-(2-{hexahydropyrrolo[3,4-*c*]pyrrol-2(1*H*)-yl}-1*H*-benzimidazol-1-yl)piperidin-1-yl]cyclooctyl}methanol, systemically potent novel non-peptide agonist of nociceptin/orphanin FQ receptor as analgesic for the treatment of neuropathic pain: design, synthesis, and structure–activity relationships, *Bioorg. Med. Chem.* **2010**, *18*, 7675–7699.

4. Hayashi, S.; Hirao, A.; Imai, A.; Nakamura, H.; Murata, Y.; Ohashi, K.; Nakata, E. Novel non-peptide nociceptin/orphanin FQ receptor agonist, 1-[1-(1-methylcyclooctyl)-4-piperidinyl]-2-[(3*R*)-3-piperidinyl]-1*H*-benzimidazole: design, synthesis, and structure–activity relationship of oral receptor occupancy in the brain for orally potent antianxiety drug, *J. Med. Chem.* **2009**, *52*, 610–625.

5. Hayashi, S.; Hirao, A.; Nakamura, H.; Yamamura, K.; Mizuno, K.; Yamashita, H. Discovery of 1-[1-(1-methylcyclooctyl)-4-piperidinyl]-2-[(3*R*)-3-piperidinyl]-1*H*-benzimidazole: integrated drug-design and structure–activity relationships for orally potent, metabolically stable and potential-risk reduced novel non-peptide nociceptin/orphanin FQ receptor agonist as antianxiety drug, *Chem. Biol. Drug Des.* **2009**, *74*, 369–381.

6. Hayashi, S.; Ohashi, K.; Nakata, E.; Emoto, C. Discovery of 1-(β-amino substituted-β-alanyl)-*N*,*N*-dimethylindoline-2-carboxamides as novel nonpeptide antagonists of nociceptin/orphanin FQ receptor: efficient design, synthesis, and structure–activity relationship studies, *Eur. J. Med. Chem.* **2012**, *55*, 228–242.

7. Hayashi, S.; Ohashi, K.; Nakata, E.; Emoto, C. Efficient design, synthesis and structure–activity relationship studies of 1-(3′-substituted propyl)-4-arylpiperidines as non-peptide antagonists of nociceptin/orphanin FQ receptor: biological activities, metabolic stabilities and hERG channel bindings, *Med. Chem. Res.* **2014**, *23*, 526–552.

8. (a) Briscini, L.; Corradini, L.; Ongini, E.; Bertorelli, R. Up-regulation of ORL-1 receptors in spinal tissue of allodynic rats after sciatic nerve injury, *Eur. J. Pharmacol.* **2002**, *447*, 59–65; (b) Mika, J.; Schäfer, M. K. H.; Obara, I.; Weihe, E.; Przewlocka, B. Morphine and endomorphin-1 differently influence pronociceptin/orphanin FQ system in neuropathic rats, *Pharmacol. Biochem. Behav.* **2004**, *78*, 171–178; (c) Chen, Y.; Sommer, C. Activation of the nociceptin opioid system in rat sensory neurons produces antinociceptive effects in inflammatory pain: involvement of inflammatory mediators, *J. Neurosci. Res.* **2007,** *85*, 1478–1488; (d) Andoh, T.; Itoh, M.; Kuraishi, Y. Nociceptin gene expression in rat dorsal root ganglia induced by peripheral inflammation, *NeuroReport* **1997**, *8*, 2793–2796; (e) Ertsey, C.; Hantos, M.; Bozsik, G.; Tekes, K., Circulating nociceptin levels during the cluster headache period, *Cephalalgia* **2004,** *24*, 280–283; (f) Devine, D. P.; Hoversten, M. T.; Ueda, Y.; Akil, H. Nociceptin/orphanin FQ content is decreased in forebrain neurons during acute stress, *J. Neuroendocrinol.* **2003**, *15*, 69–74; (g) Delaney, G.; Dawe, K. L.; Hogan, R.; Hunjan, T.; Roper, J.; Hazell, G.; Lolait, S. J.; Fulford, A. J. Role of nociceptin/orphanin FQ and NOP receptors in the response to acute and repeated restraint stress in rats, *J. Neuroendocrinol.* **2012,** *24*, 1527–1541; (h) Reiss, D.; Wolter-Sutter, A.; Krezel, W.; Ouagazzal, A.-M. Effects of social crowding on emotionality and expression of hipocampal nociceptin/orphanin FQ system transcripts in mice, *Behav. Brain Res.* **2007**, *184*, 167–173; (i) Rodi, D.; Polidori, C.; Bregola, G.; Zucchini, S.; Simonato, M.; Massi, M. Pro-nociceptin/orphanin FQ and NOP receptor mRNA levels in the forebrain of food deprived rats, *Brain Res.* **2002,** *957*, 354–361; (j) Kuzmin, A.; Bazov, I.; Sheedy, D.; Garrick, T.; Harper, C.; Bakalkin, G. Expression of pronociceptin and its receptor is downregulated in the brain of human alcoholics, *Brain Res.* **2009,** *1305, Suppl.*, S80–S85; (k) Neal, C. R. Jr.; Akil, H.; Watson, S. J. Jr. Expression of orphanin FQ and the opioid receptor-like (ORL1) receptor in the developing human and rat brain, *J. Chem. Neuroanat.* **2001**, *22*, 219–249; (l) Buzas, B.; Rosenberger, J.; Cox, B. M., Activity and cyclic AMP-dependent regulation of nociceptin/orphanin FQ gene expression in primary neuronal and astrocyte cultures, *J. Neurochem.* **1998,** *71*, 556–563; (m) Buzas, B.; Symes, A. J.; Cox, B. M., Regulation of nociceptin/orphanin FQ gene expression by neuropoietic cytokines and neurotrophic factors in neurons

and astrocytes, *J. Neurochem.* **1999,** *72*, 1882–1889; (n) Miller, T. R.; Fulford, A. J., Regulation of nociceptin/orphaninFQ secretion by immune cells and functional modulation of interleukin-2, *Peptides* **2007,** *28*, 2243–2252; (o) Sinchak, K.; Romeo, H. E.; Micevych, P. E. Site-specific estrogen and progestin regulation of orphanin FQ/nociceptin and nociceptin opioid receptor mRNA expression in the female rat limbic hypothalamic system, *J. Comp. Neurol*. **2006**, *496*, 252–268.

9. Inoue, H.; Matsunaga, S.; Rashid, M. H.; Yoshida, A.; Mizuno, K.; Sakurada, T.; Takeshima, H.; Ueda, H. Pronociceptive effects of nociceptin/orphanin FQ (13–17) at the peripheral and spinal level in mice, *J. Pharmacol. Exp. Ther.* **2001**, *299*, 213–219.

10. Watanabe, H.; Mizoguchi, H.; Orito, T.; Katsuyama, S.; Yonezawa, A.; Watanabe, C.; Sakurada, T.; Sakurada, S. Possible involvement of endogenous nociceptin/orphanin FQ in the pain-related behavioral responses induced by its own metabolite, nociceptin/orphanin FQ(14–17), *Peptides* **2007**, *28*, 670–677.

11. Sakurada, T.; Komatsu, T.; Moriyama, T.; Sasaki, M.; Sanai, K.; Orito, T.; Sakurada, C.; Sakurada, S. Effects of intraplantar injections of nociceptin and its N-terminal fragments on nociceptive and desensitized responses induced by capsaicin in mice, *Peptides* **2005**, *26*, 2505–2512.

12. Katsuyama, S.; Mizoguchi, H.; Komatsu, T.; Sakurada, C.; Tsuzuki, M.; Sakurada, S.; Sakurada, T. Antinociceptive effects of spinally administered nociceptin/orphanin FQ and its *N*-terminal fragments on capsaicin-induced nociception, *Peptides* **2011**, *32*, 1530–1535.

13. Terenius, L.; Sandin, J.; Sakurada, T. Nociceptin/orphanin FQ metabolism and bioactive metabolites, *Peptides* **2000**, *21*, 919–922.

14. Bigoni, R.; Calo, G.; Guerrini, R.; Strupish, J. W.; Rowbotham, D. J.; Lambert, D. G. Effects of nociceptin and endomorphin 1 on the electrically stimulated human vas deferens, *Br. J. Clin. Pharmacol.* **2001,** *51*, 355–358.

15. Gavioli, E. C.; Marzola, G.; Guerrini, R.; Bertorelli, R.; Zucchini, S.; De Lima, T. C. M.; Rae, G. A.; Salvadori, S.; Regoli, D.; Calo, G. Blockade of nociceptin/orphanin FQ–NOP receptor signalling produces antidepressant-like effects: pharmacological and genetic evidences from the mouse forced swimming test, *Eur. J. Neurosci.* **2003**, *17*, 1987–1990.

16. Chee, M. J.; Price, C. J.; Statnick, M. A.; Colmers, W. F., Nociceptin/orphanin FQ suppresses the excitability of neurons in the ventromedial nucleus of the hypothalamus, *J. Physiol.* **2011,** *589*, 3103–3114.

17. Economidou, D.; Policani, F.; Angellotti, T.; Massi, M.; Terada, T.; Ciccocioppo, R. Effect of novel NOP receptor ligands on food intake in rats, *Peptides* **2006**, *27*, 775–783.

18. Hashiba, E.; Hirota, K.; Kudo, T.; Calo', G.; Guerrini, R.; Matsuki, A. Effects of nociceptin/orphanin FQ receptor ligands on blood pressure, heart rate, and plasma catecholamine concentrations in guinea pigs, *Naunyn-Schmiedeberg's Arch. Pharmacol.* **2003**, *367*, 342–347.

19. (a) Narita, M.; Mizoguchi, H.; Oji, D. E.; Narita, M.; Dun, N. J.; Hwang, B. H.; Nagase, H.; Tseng, L. F. Identification of the G-protein-coupled ORL1 receptor in the mouse spinal cord by [^{35}S]GTPγS binding and immunohistochemistry, *Br. J. Pharmacol.* **1999**, *128*, 1300–1306; (b) Review: MacPherson, R. D. New directions in pain management, *Drugs Today* **2002**, *38*, 135–145; (c) Review: Zöllner C.; Stein, C. Opioids. In *Analgesia*; Stein, C., Ed.; Handbook of Experimental Pharmacology; Vol 177; Springer-Verlag GmbH: Berlin Heidelberg, Germany, **2006**, pp 31–63; (d) Varrassi, G.; Angeletti, C.; Guetti, C.; Marinangeli, F.; Paladini, A., Systemic opioid and chronic pain, *Eur. J. Pain Suppl.* **2009,** *3*, 77–83.

20. Gibson, S. E.; Guillo, N.; Kalindjian, S. B.; Tozer, M. J. Incorporation of conformationally constrained phenylalanine derivatives Tic, Sic, Hic and Nic into a cholecystokinin-B/gastrin receptor antagonist, *Bioorg. Med. Chem. Lett.*, **1997**, *7*, 1289–1292.

21. Romero, A. G.; Leiby, J. A.; Mizsak, S. A. Synthesis of an azasteroid using acyl iminium ion-initiated tandem cyclization, *J. Org. Chem.* **1996**, *61*, 6974–6979.

22. McKenna, J. M.; Moliterni, J.; Qiao, Y. The scope and limitations of the Suzuki–Miyaura cross-coupling reactions of 6- and 8-substituted 1,2,3,4-tetrahydroisoquinoline-3-carboxylates, *Tetrahedron Lett.* **2001**, *42*, 5797–5800.

23. Vicente, T.; Martinez de Marigorta, E.; Domínguez, E.; Carrillo. L.; Badia, D. A new route towards 8-oxoprotoberberines, *Heterocycles* **1993**, 36, 2067–2072.

24. Ornstein, P. L.; Arnoldo, M. B.; Augenstein, N. K.; Paschal, J. W. Syntheses of 6-oxodecahydroisoquinoline-3-carboxylates. Useful intermediates for the preparation of conformationally defined excitatory amino acid antagonists, *J. Org. Chem.* **1991**, *56*, 4388–4392.

25. Cheng Y.-C.; Prusoff, W. H. Relationship between the inhibition constant (K_i) and the concentration of inhibitor which causes 50 per cent inhibition (I_{50}) of an enzymatic reaction, *Biochem. Pharmacol.* **1973**, *22*, 3099–3108.

26. Moulédous, L.; Topham, C. M.; Mazarguil, H.; Meunier, J.-C. Direct identification of a peptide binding region in the opioid receptor-like 1 receptor by photoaffinity labeling with [Bpa^{10},Tyr^{14}]nociceptin. *J. Biol. Chem.* **2000**, *275*, 29268–29274.

27. Mollereau, C.; Mouledous, L.; Lapalu, S.; Cambois, G.; Moisand, C.; Butour, J.-L. Meunier, J.-C. Distinct mechanisms for activation of the opioid receptor-like 1 and κ-opioid receptors by nociceptin and dynorphin A. *Mol. Pharmacol.* **1999**, *55*, 324–331.

28. Dooley, C. T.; Spaeth, C. G.; Berzetei-Gurske, I. P.; Craymer, K.; Adapa, I. D.; Brandt, S. R.; Houghten, R. A.; Toll, L. Binding and *in vitro* activities of peptides with high afinity for the nociceptin/orphanin FQ receptor, ORL1. *J. Pharmacol. Exp. Ther.* **1997**, *283*, 735–741.

29. Kawano, M.; Okada, K.; Honda, T.; Nose, T.; Sakaguchi, K.; Costa, T.; Shimohigashi, Y. Structural requirement of nociceptin antagonist Ac-RYYRIK-NH_2 for receptor binding. *J. Pept. Sci.* **2002**, *8*, 561–569.

30. Mouledous, L.; Topham, C. M.; Moisand, C.; Mollereau, C.; Meunier, J.-C. Functional inactivation of the nociceptin receptor by alanine substitution of glutamine 286 at the C terminus of transmembrane segment VI: evidence from a site-directed mutagenesis study of the ORL1 receptor transmembrane-binding domain. *Mol. Pharmacol.* **2000**, *57*, 495–502.

31. Kam, K. W. L.; New, D. C.; Wong, Y. H. Constitutive activation of the opioid receptor-like (ORL_1) receptor by mutation of Asn133 to tryptophan in the third transmembrane region. *J. Neurochem.* **2002**, *83*, 1461–1470.

32. Thompson, A. A.; Liu, W.; Chun, E.; Katritch, V.; Wu, H.; Vardy, E.; Huang, X.-P.; Trapella, C.; Guerrini, R.; Calo, G.; Roth, B. L.; Cherezov, V.; Stevens, R. C. Structure of the nociceptin/orphanin FQ receptor in complex with a peptide mimetic. *Nature*, **2012**, *485*, 395–401.

33. Orsini, M. J.; Nesmelova, I.; Young, H. C.; Hargittai, B.; Beavers, M. P.; Liu, J.; Connolly, P. J.; Middleton, S. A.; Mayo, K. H. The nociceptin pharmacophore site for opioid receptor binding derived from the NMR structure and bioactivity relationships. *J. Biol. Chem.* **2005**, *280*, 8134–8142.

34. Reinscheid, R. K.; Ardati, A.; Monsma, F. J., Jr.; Civelli, O. Structure–activity relationship studies on the novel neuropeptide orphanin FQ. *J. Biol. Chem.* **1996**, *271*, 14163–14168.

Scheme Legends

Scheme 1 Synthesis of compound **5**. Reagents and conditions: (a) WSCI, HOBT, Et_3N, CH_2Cl_2; (b) 10% HCl/MeOH; (c) LAH, THF, 0 °C to room temp.

Scheme 2 Synthesis of compound **15.** Reagents and conditions: (a) NaH, DMF, 0 °C to room temp; (b) 0 °C to room temp; (c) concd HCl, AcOH, reflux; (d) formalin, H_2O, 90 °C; (e) Boc_2O, 2 N NaOH, 1,4-dioxane; compound **12**, see text; (f) WSCI, HOBT, Et_3N, CH_2Cl_2; (g) TFA, THF, 0 °C to room temp; (h) $BH_3 \cdot SMe_2$, THF, room temp to reflux.

Scheme 3 Synthesis of compounds **18**, **19**, **20**, **21**, and **22**. Reagents and conditions: (a) WSCI, HOBT, Et_3N, DMF–THF, –20 °C to room temp; (b) 10% HCl/MeOH; (c) LAH, THF, 0 °C to room temp; (d) LAH, THF; (e) $KMnO_4$, $MgSO_4$, acetone–H_2O; (f) AcCl, Et_3N, CH_2Cl_2, room temp to reflux.

Scheme 4 Synthesis of compounds **23** and **25**.

Scheme 5 Synthesis of compounds **27** and **30**. Reagents and conditions: (a) Boc_2O, 2 N NaOH, 1,4-dioxane; (b) H_2 (1–4 atm), 5% Pd/C, MeOH; (c) 10% HCl/MeOH; (d) Boc_2O, Na_2CO_3, 1,4-dioxane–H_2O; (e) WSCI, HOBT, Et_3N, DMF.

Scheme 6 Synthesis of compounds **33**. Reagents and conditions: (a) WSCI, HOBT, Et_3N, DMF; (b) LAH, THF, 0 °C to room temp.

Scheme 7 High-speed parallel synthesis of compounds **36** and **38**. Reagents and conditions: (a) Et_3N, 1,2-dichloroethane, then filtration; (b) i) LAH, Et_2O–THF; ii) H_2O, 10% MeOH–CH_2Cl_2; iii) Na_2SO_4–SiO_2 column.

Scheme 8 Design of 3-{[4-(4-fluoro-2-methylphenyl)piperidin-1-yl]methyl}-tetrahydroisoquinoline analogs **41**.

Tables

Table 1: Structure–activity relationships of binding affinities to human recombinant NOP receptor and human recombinant μ receptor *in vitro* and antagonist activities against human recombinant NOP receptor *in vitro* for (4-arylpiperidine substituted-methyl)-[bicyclic (hetero)cycloalkanobenzene] analogs.[a]

	Compounds: R^1–R^2		*In vitro*			
			Human NOP receptor binding[b]	Human μ receptor binding[b]	Selectivity ratio of receptor binding	Antagonism against N/OFQ-stimulated [^{35}S]GTPγS binding[d]
No	R^1–	R^2–	K_i (nM)	K_i (nM)	μ /NOP[c]	IC_{50} (nM)
5	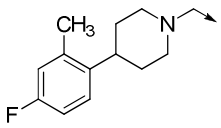	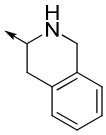	3.56	342	96.1	58.8
15	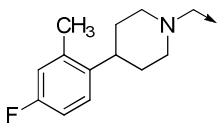	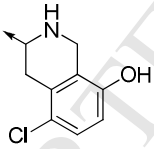	3.13	>450	>143	28.7
18	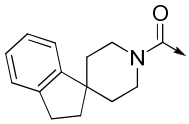	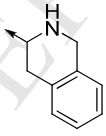	>250	>450	–	NT[e]
19	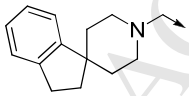	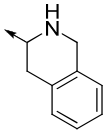	8.50	225	26.5	248
20	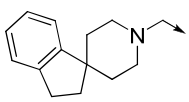	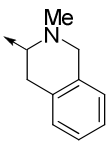	18.9	58.2	3.08	NT

21	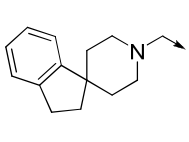	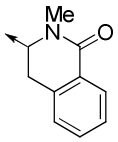	>250	231	<0.924	NT
22	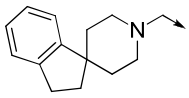	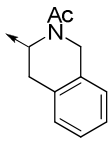	29.8	74.4	2.50	NT
23	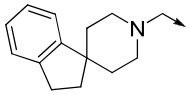	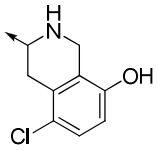	2.20	68.8	31.3	21.3
25	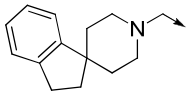	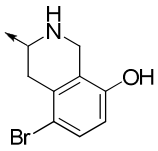	1.74	139	79.9	35.1
27	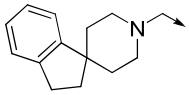	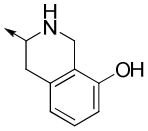	2.40	288	120	53.9
30	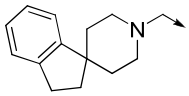	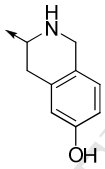	10.2	392	38.4	227
33	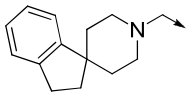	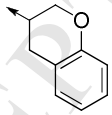	5.65	49.1	8.69	122
38	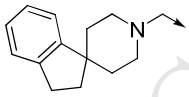	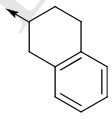	5.55	289	52.1	683

[a] Compounds **5**, **15**, **18**–**23**, **25**, **27**, **30**, and **33**: prepared by manual synthesis; compound **38**: prepared by high-speed parallel synthesis.

[b] K_i values for compounds were measured by displacement of [^{3}H]N/OFQ binding to hNOP receptor expressed in HEK-293 cells and of [^{3}H]DAMGO binding to human μ receptor expressed in CHO-K1 cells, respectively. $K_i = IC_{50}/(1+[\text{radioligand}]/K_D)$. Radioligands: [^{3}H]N/OFQ as hNOP receptor agonist, concentration 0.4 nM, K_D = 0.135 nM; [^{3}H]DAMGO as human μ receptor agonist, concentration 1.0 nM, K_D = 0.821 nM.

[c] The selectivities of hNOP receptor antagonists against human μ receptor were calculated as the ratios of the K_i values for human μ receptor to the K_i values for hNOP receptor.

[d] Antagonism IC_{50} values for compounds were measured as inhibitory activity against [^{35}S]GTPγS binding to α-unit of G-protein due to binding of N/OFQ to hNOP receptor expressed in HEK-293 cells.

[e] NT, not tested.

Table 2: Structure–metabolic stability relationships of half-lives in human liver microsome and structure–activity relationships of hERG channel binding affinities *in vitro* for (4-arylpiperidine substituted-methyl)-[bicyclic (hetero)cycloalkanobenzene] analogs.[a]

Compounds: R^1–R^2			Half-life in HLM[b]	hERG channel binding *in vitro*[c]
No	R^1–	R^2–	min	IC_{50} (nM)
5	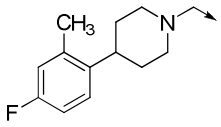	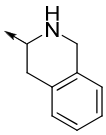	6.9	200
15	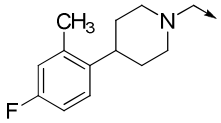	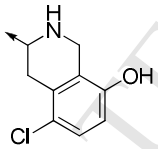	21.6	970
19	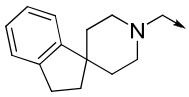	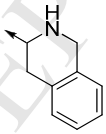	6.6	>1,500
21	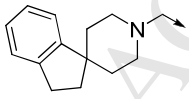	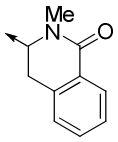	NT[d]	6,960
22	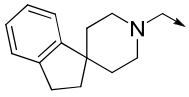	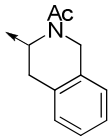	NT	500

23	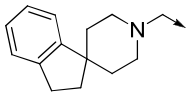	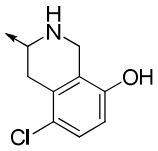	15.3	1,730
25	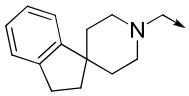	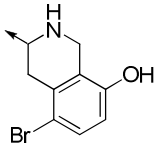	9.6	1,000
27	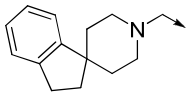	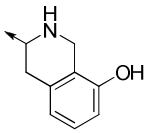	12.2	940
30	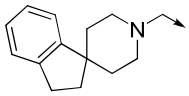	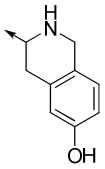	18.0	340
33	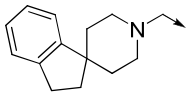	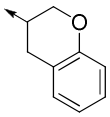	3.1	1,500
38	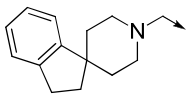	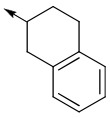	NT	71% @1 μM

[a] Compounds **5**, **15**, **19**, **21**–**23**, **25**, **27**, **30**, and **33**: prepared by manual synthesis; compound **38**: prepared by high-speed parallel synthesis.

[b] Half-lives of these compounds in human liver microsome were measured by HPLC/MS/MS.

[c] IC_{50} values for these compounds were measured by displacement of [^{3}H]dofetilide binding to potassium channel from hERG products expressed in HEK-293 cells.

[d] NT, not tested.

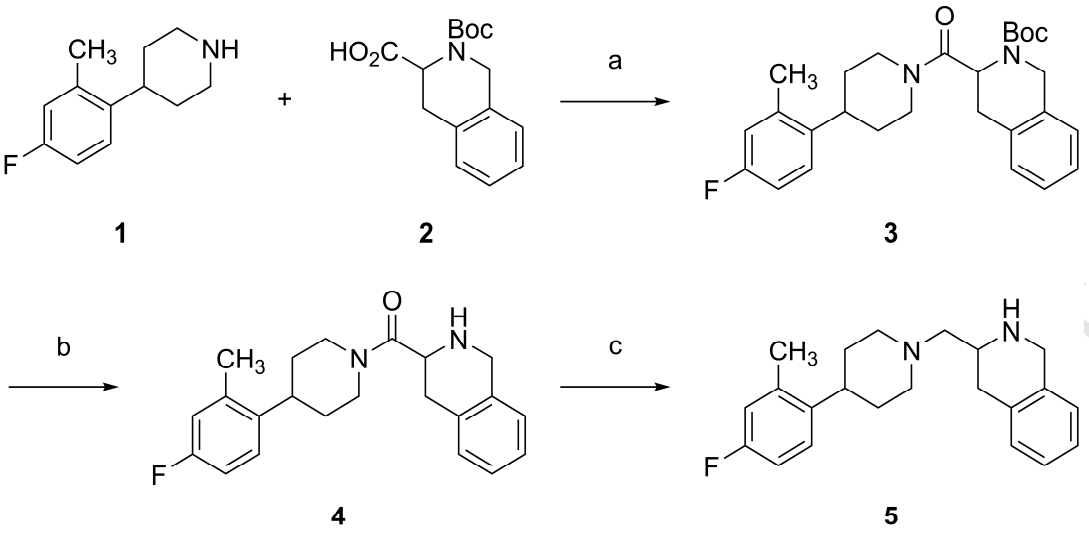

1 **2** **3**

4 **5**

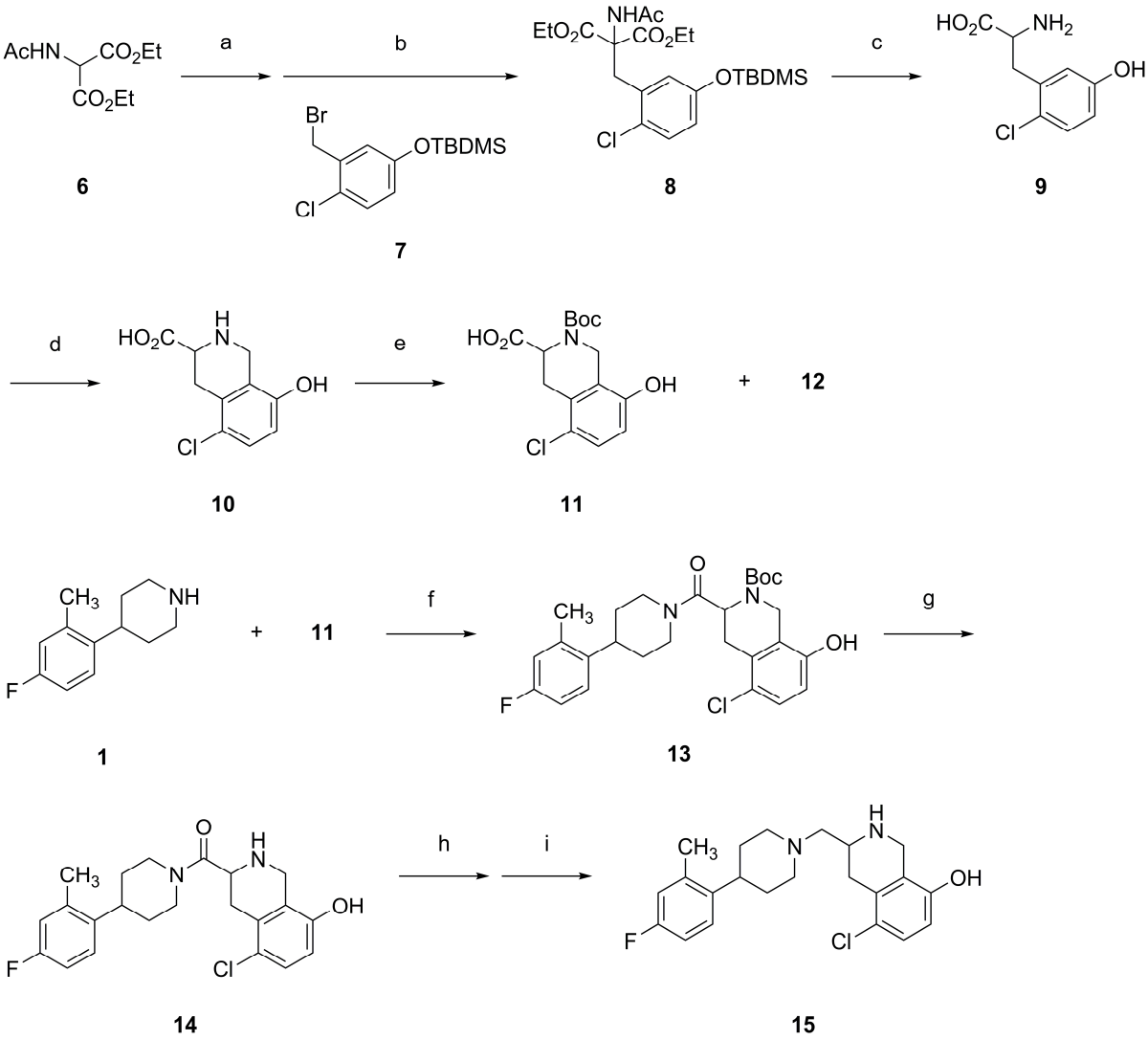
AcHN
CO2Et
CO2Et
a
b
Br
OTBDMS
Cl
EtO2C
NHAc
CO2Et
OTBDMS
Cl
c
HO2C
NH2
OH
Cl
6
7
8
9
d
HO2C
H
N
OH
Cl
e
HO2C
Boc
N
OH
Cl
+
12
10
11
CH3
NH
F
+
11
f
CH3
O
Boc
N
N
OH
F
Cl
g
1
13
CH3
O
H
N
N
OH
F
Cl
h
i
CH3
N
H
N
OH
F
Cl
14
15

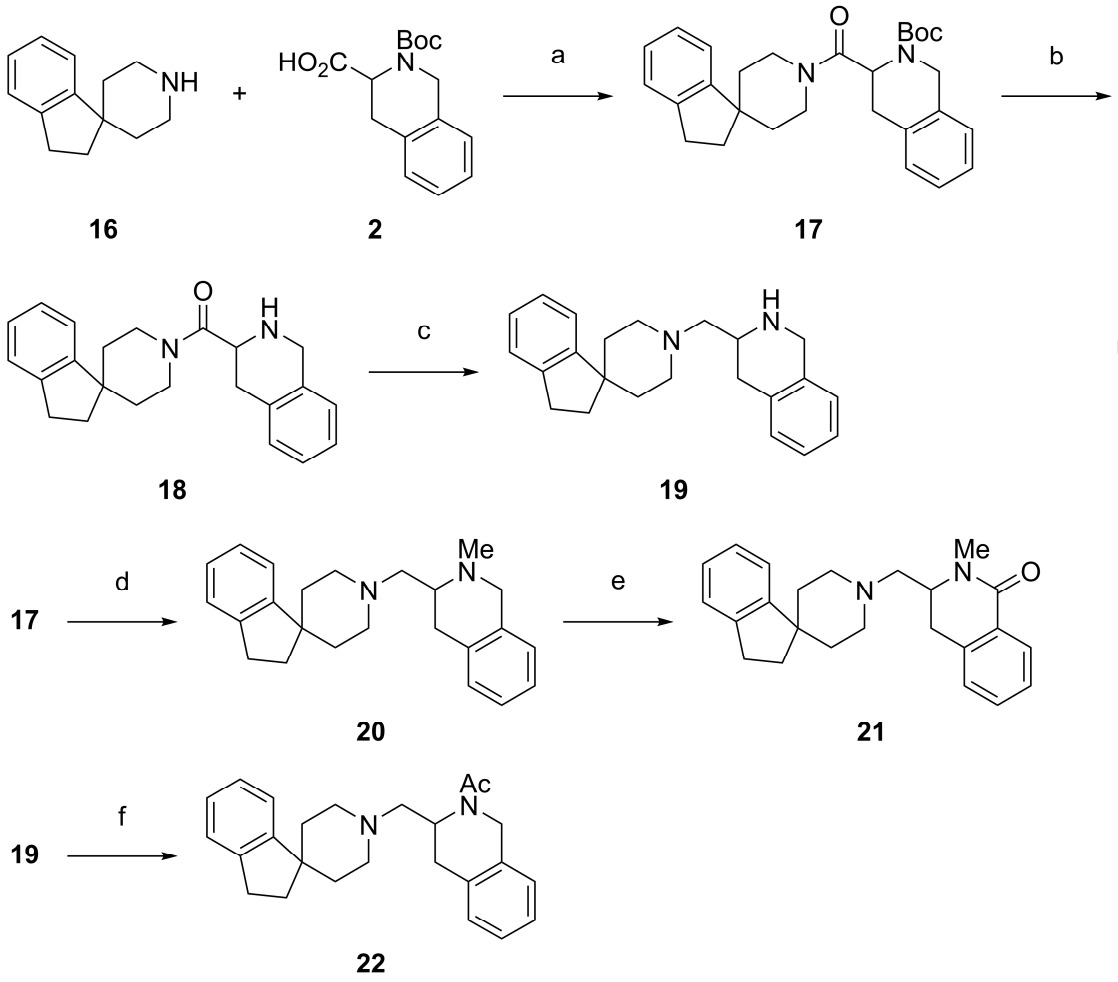
NH
+
HO2C
Boc
N
a
O
Boc
N
N
b
16
2
17
O
H
N
N
c
18
H
N
N
19
17
d
Me
N
N
e
Me
N
N
O
20
21
19
f
Ac
N
N
22

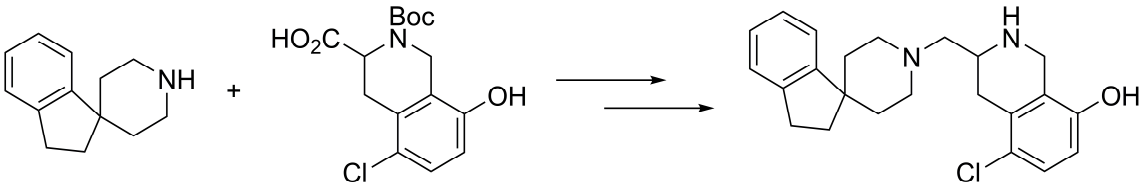

16 **11** **23**

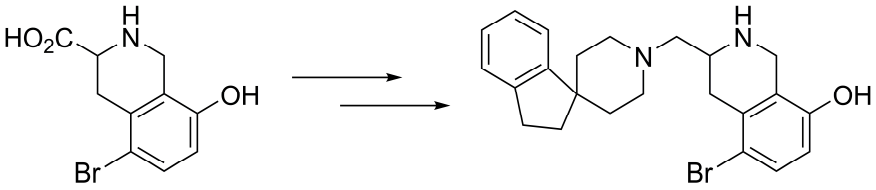

24 **25**

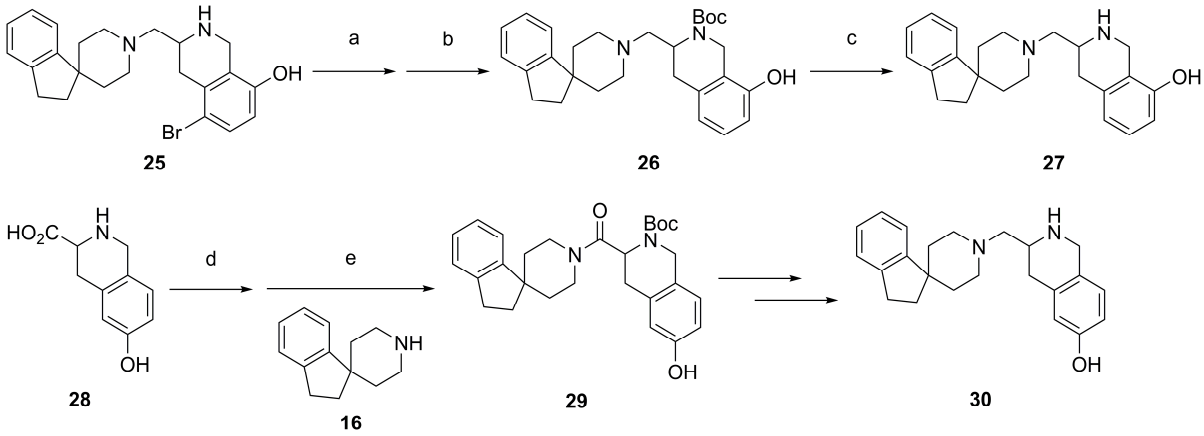

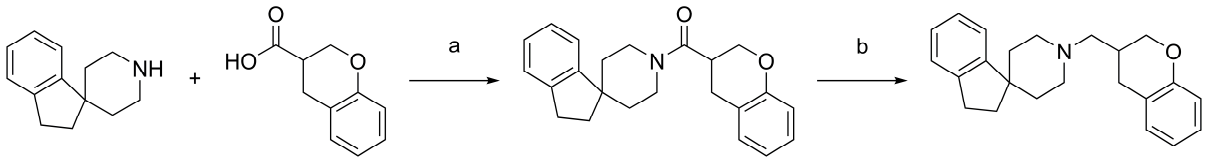

16 **31** **32** **33**

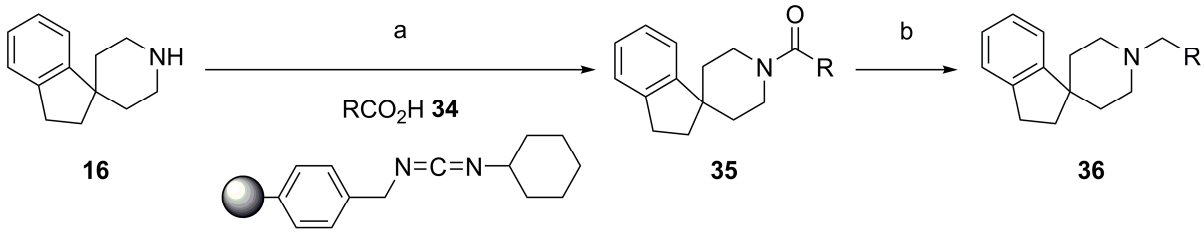

16 35 36

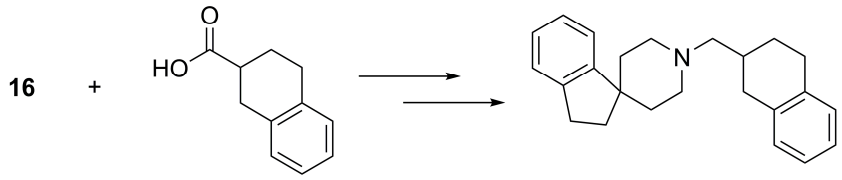

37 38

Hayashi, et al. [6]

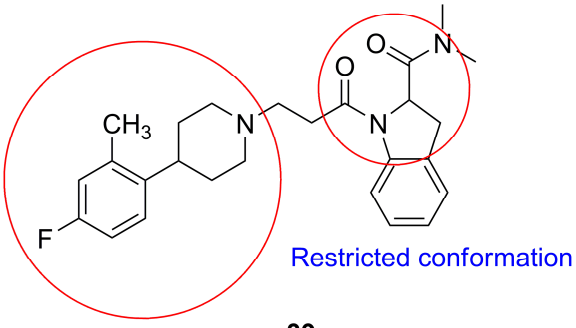

Restricted conformation

Preferable unit

39

Hayashi, et al. [7]

Smaller and simpler structure

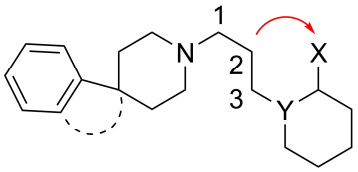

X = CH_3 or H

Y = N or CH

Monocyclic unit with three-carbon linker

40

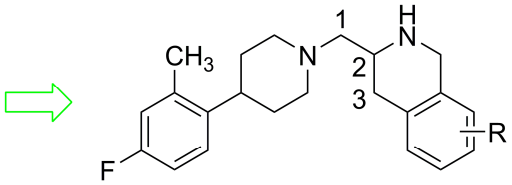

41

cf.

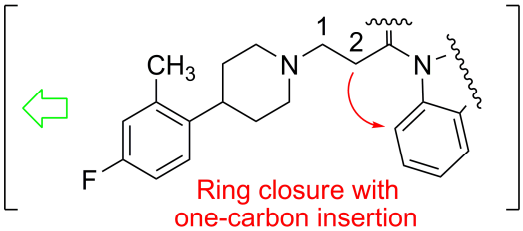

39′

Novel hNOP receptor antagonists

The highlights of this article are as follows:

- Novel small-molecule NOP receptor antagonists were designed, prepared, and evaluated.
- Compound **15** exhibited high potency and high selectivity as a NOP receptor antagonist.
- Contributing-factors for potency/selectivity of NOP receptor antagonist are suggested.
- Contributing-factors for metabolic stability are suggested.
- Contributing-factors for reducing hERG channel binding affinity are suggested.